Functionalised biochar for fire-retardant & bio-based composites

Oisik Das
Rhoda Afriyie Mensah

BRANDFORSK
2022:7

BRAND FORSK

Brandforsk republishes the project report from LTU, that is published on their website www.ltu.se for reference

”Functionalised biochar for fire-retardant & bio-based composites”

BRANDFORSK

2022:7

Brandforsk’s activities are made possible by support from various organizations in the community. Read more about our support organisations at www.brandforsk.se

Functionalised biochar for fire-retardant and bio-based composites

Final Report for Project number: 321-002

Funded Application to Brandforsk, May 2021
By: Oisik Das (LTU)
Research Team: Oisik Das (project leader) and Rhoda A Mensah (postdoc)

Abstract:
Although flame/fire retardants are very effective in reducing the fire hazard of polymeric materials, their presence in the resin matrix may be detrimental to mechanical strength. Hence, in order to have a holistic improvement of performance properties, a new approach has been developed wherein biochar pores are used to host fire retardants. The issue of loss in mechanical strength of a polymer host is alleviated by the use of reinforcing biochar whereas the fire-safety is enhanced by the presence of the fire retardants. Initially, three different doping procedures were investigated, namely, dry mixing, and chemical and thermal-based doping, to integrate fire retardant into the biochar pores. The doped biochar was used to develop bioplastic-based composites. The mechanical and flammability properties of the composites were assessed. It was found that thermal doping was the most effective in introducing significant amounts of fire-retardant particles inside the biochar pores. The bioplastic containing thermally doped biochar had tensile strength, which was comparable to that of the unmodified material. The thermally doped biochar composites displayed low cone calorimeter peak heat release rate for combustion and the high apparent activation energy for decomposition. However, a comparison between fire retardants (lanosol and ammonium polyphosphate), bioplastics (wheat gluten and polyamide 11) and composite processing methods (compression and injection moulding) revealed that doped ammonium polyphosphate in gluten made by compression moulding has the best fire-safety properties with the lowest peak heat release rate (186 kW/m^2) with acceptable mechanical properties compared to the unmodified bioplastic. However, the doped lanosol in gluten made by compression moulding has an overall acceptable fire and mechanical properties compared to the corresponding neat bioplastic. Thus, for gluten-based polymer matrices, the use of fire-retardant additives thermally doped into biochar made by compression moulding is recommended to both simultaneously improve fire-safety and conserve mechanical strength.

Scientific articles published and/or in preparation from this project:
Published: Perroud, T., Shanmugam, V., Mensah, R.A., Jiang, L., Xu, Q., Neisiany, R.E., Sas, G., Försth, M., Kim, N.K., Hedenqvist, M.S. and Das, O., 2022. Testing bioplastics containing functionalised biochar. Polymer Testing, p.107657.

In preparation: Das, O., Mensah, R.A., Försth, M., Shanmugam, V., 2022. Functionalised biochar with APP: The effect of bioplastics and processing methods. To be submitted to Composites Part C.

Background:
The growing concern about the environmental hazards of synthetic materials necessitates the development and use of biobased materials [1-3]. The development of biobased plastics and composites has accelerated in recent years [4-8]. Biocomposites have the potential to replace fossil-based composites in a wide range of items, including aeroplane and automotive parts, furniture, packaging, building materials, implants, and household appliances [9-13]. However, polymers, including biobased ones have some drawbacks that limit their application, for instance, poor fire resistance and thermal behaviour [14-17]. In biocomposites, both the reinforcement and matrix are susceptible to degradation by fire. Typically, the reinforcement in biocomposites may be a fibre or biomass that degrades at relatively low temperatures (ca. 200 °C) that negatively affects the bonding with the polymeric matrix [18, 19]. The matrix material also undergoes thermally induced changes and degradation, often at even lower temperatures than the fibres/biomass (e.g., polypropylene starts melting at ca. 160 °C). However, protein-based matrices are slightly less prone to burning as compared to their synthetic counterparts but may still lose structural integrity during and post-fire heat exposure [20]. In fact, there is a dearth of knowledge about the flammability of protein-based bioplastics. In order to employ bioplastics for composite development, it is imperative that they undergo fire-retarding treatments. Moreover, a fire-resistant replacement for biomass/natural fibres should also be identified.

Often, the application of fire-retardant (FR) treatments (non-halogenated) in biocomposites creates unintended and detrimental consequences [21, 22] such as a reduction in mechanical strength [23, 24]. The microscopic presence of FR particles can act as stress concentration points that lead to a decrease in the tensile strength of the material [25]. Poor dispersion of FR particles and their incompatibility with the polymer matrix is also unfavourable for the retention of good mechanical properties [26]. It is desirable to achieve holistic improvement in the performance properties of the developed biocomposites. Hence, FR treatments should therefore be aimed at conserving or even improving the mechanical properties along with imparting fire resistance. It is desirable to apply FR treatments for the biocomposite constituents before the manufacturing process to avoid the aforementioned issues. In this regard, graphene sheets, silica nanoparticles, and biochar have been reported to create a balance between the mechanical and flammability properties of plastics [27, 28].

Biochar, which is the solid pyrolysis product of biomass [29-31], having a stable carbon main chain, porous honeycomb structure, and lacking flammable volatiles, is reported to have acceptable fire resistance, thermal stability as well as the ability to enhance composites' mechanical performance [32, 33]. The numerous pores in the biochar's surface facilitate the flow of molten polymer into the particles during processing and thus, create a mechanical interlocking, which may enhance mechanical properties [34]. Biochar has been identified as a potent reinforcement for composite materials that may also improve fire resistance [20]. However, the fire resistance that biochar bestows is purely of additive nature and is solely dependent on the loading amount contained inside the polymer. Additionally, biochar containing polymers have not been reported to display a V-0 rating in UL-94 vertical burn tests and do not possess significantly higher limiting oxygen indices than those observed for the unmodified polymeric material [21]. The advent of biopolymers such as wheat gluten (WG) and polyamide 11 (PA 11) bioplastics has helped to reduce environmental footprints globally. Wheat gluten has been used as a matrix in biocomposites containing biochar as reinforcement. On the other hand, PA 11 is extensively used in tubing,

electrical covers, and also in textiles. Polylactide (PLA) was not readily available for this current project in a ground form and hence, PA 11 was used, which has a more widespread application than PLA, apart from also being a bioplastic. Lanosol is a naturally occurring flame retardant obtained from red algae [35]. Lanosol functions by releasing free radicals mostly in the gas phase of the wheat gluten's combustion and hinder the chemical reactions happening within the flame. In this particular FR, characteristic atoms are released that remove high-energy H and OH radicals formed during combustion. The quenching of the flame's chemical reactions can lead to the reduction of heat release rate and fire spread [35]. It should be noted that the optimal amount of lanosol required for improved flame retardancy is 4 wt.%. The usage of small quantities consequently reduces the amount of HBr released compared to other halogenated FR's which require 10 wt.%. The integration of lanosol to biochar and wheat gluten further reduces the HBr content since the char formed by the WG controls the emission of gases. Ammonium polyphosphate (APP) is a potent and widely used FR, which is considered to be benign to human health and possesses very low environmental impact. APP is an intumescent FR, which functions in the condensed phase system in a polymer matrix and capitalises the phosphorous-nitrogen synergy.

Doping of fire-retardant treatments have been used to take advantage of the synergistic effects of multiple fire retardants. In the work of Attia [36], polypyrrole nanoparticles were doped with phosphoric acid to study the thermal and fire behaviour at different loading amounts. Significant improvements were seen in the flammability of the doped samples, however, the effect of the doping on the mechanical properties of the samples was not determined. In light of the aforementioned, the overarching aim of this project was to treat a composite constituent with an optimal FR system (i.e. lanosol or APP-based) and to use the same to manufacture biocomposites with an optimal manufacturing process and polymer that are both fire-retardant and mechanically strong. The first step was to treat biochar individually with lanosol as the FR to create a 'fire-retardant biochar', which is an upgradation from merely 'fire-resistant biochar.' In fact, the doped biochar will act as a FR delivery vehicle (i.e., functionalised biochar) into the bioplastic's matrix. This is an important novelty consideration because the biochar would trap the FR particles in its numerous pores and enable them to react appropriately under fire when added to the bioplastic to create a composite. Being housed inside biochar pores, the FR particles can be effective in reducing the fire hazard without acting as stress concentration points in the bioplastic matrix. This would simultaneously facilitate the capitalisation of the FR's advantage (i.e., reducing flame growth) and circumventing its disadvantage (i.e., lowering of mechanical properties). With this motivation, three different methods have been developed in this investigation to introduce the FR into the biochar pores, which was followed by composite manufacturing by two different processing techniques (i.e. compression and injection moulding) containing two different bioplastics (i.e. WG and PA 11). The biocomposites were tested for their fire and mechanical properties. The report is divided into two parts wherein in the first, lanosol was doped in biochar using various mechanisms and them mixed with WG followed by fire and mechanical testing and kinetic analysis. The second part of the report describes the comparison between the two FRs (lanosol and APP) using the selected doping method from the first part as well, as the comparison between two bioplastics (WG and PA 11) with the selected doping method and the FR and finally, the assessment of two processing techniques (compression and injection moulding) with the selected doping method, FR, and the bioplastic. Finally, a composite having the most desirable doping method, FR, bioplastic and made using a suitable processing method was identified.

Part 1: Investigation of doping methods and resulting fire, mechanical and thermal kinetic properties

1. Experimental:

1.1 Materials:

Biochar was prepared from pine bark in a batch reactor at pyrolysis temperature of 800 °C for a residence time of 1 h, the details of which are explained in a previous article [32]. The biochar was ground to ca. ≤ 150 µm using ZM 200 granulator. Wheat gluten (WG) having a gluten protein content of 86.3 ± 0.3 (Dumas method, NMKL 6:2003, USA, N x 6.25) was obtained from Lantmännen Reppe AB, Sweden. The fat content was 0.9 ± 0.1 % (2009/152/EU mod) and the ash content was 0.8 ± 0.1 %, (NMKL 173). Glycerol (99 % purity) was purchased from PWG Produkter AB, Sweden and 25 % was used to plasticise the WG, based on the gluten/glycerol content. Lanosol (2,3-dibromo-4,5-dihydroxybenzyl alcohol) as a flame retardant was procured from AApin Chemicals Limited, UK.

1.2 Doping methods:

The primary goal of this study was to integrate lanosol into biochar pores and investigate the synergistic effect of flame retardant lanosol and biochar on WG-based composites. Lanosol was doped into biochar pores using three different methods: dry mix (mechanical doping), thermal and chemical doping. In all three methods, 4 wt.% of the lanosol was doped into 6 wt.% of the biochar. Fig. 1 shows the schematic representation of three different doping methods employed.

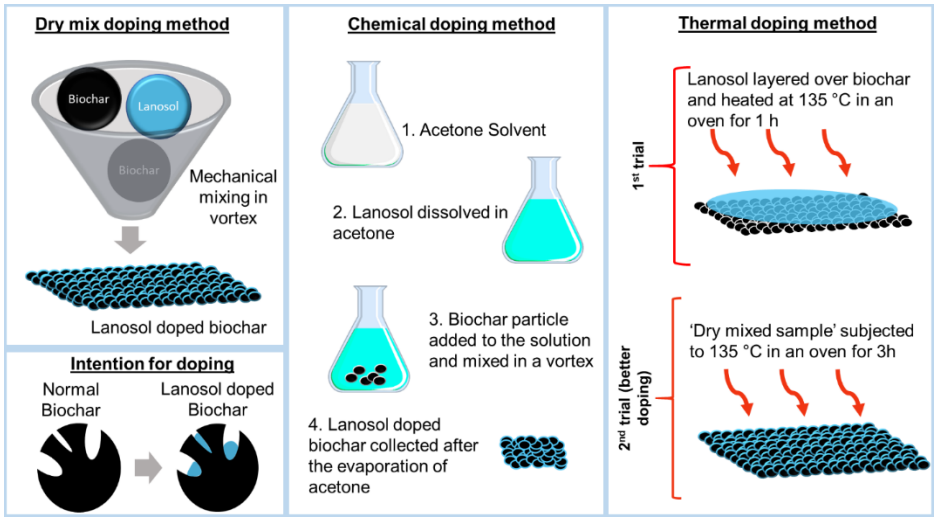

Fig. 1: Schematic representation of doping methods.

In the dry mix process, the biochar and lanosol particles were mechanically mixed (without any solvent) in a vortex mixer for 10 min. The scanning electron micrograph (method explained subsequently, *section 2.4.3*) shows an acceptable doping of lanosol in biochar particles, Fig. 2a although a considerable amount remained on the biochar's surface. In the chemical doping process, lanosol was dissolved in the acetone (solvent). Then, the biochar was added to the solution and mixed in the vortex mixer for 10 min. The acetone was allowed to evaporate, leaving the lanosol-doped biochar. From Fig. 2b, a 'coating' of lanosol can be seen over and inside the pores of the biochar particles. For thermal doping, first the biochar was placed in the tray and a thin layer of

lanosol particles was placed over it and heated at 135 °C for 1 h. In this process, it was observed that lanosol particles aggregated on the top side of the biochar (Fig. 2c), hence, the doping efficiency was deemed to be low. To address this issue, the dry mixed sample was directly used, which was placed in the oven and heated to 135 °C for 3 h. This method effectively doped the lanosol particle into the pores of the biochar (Fig. 2d).

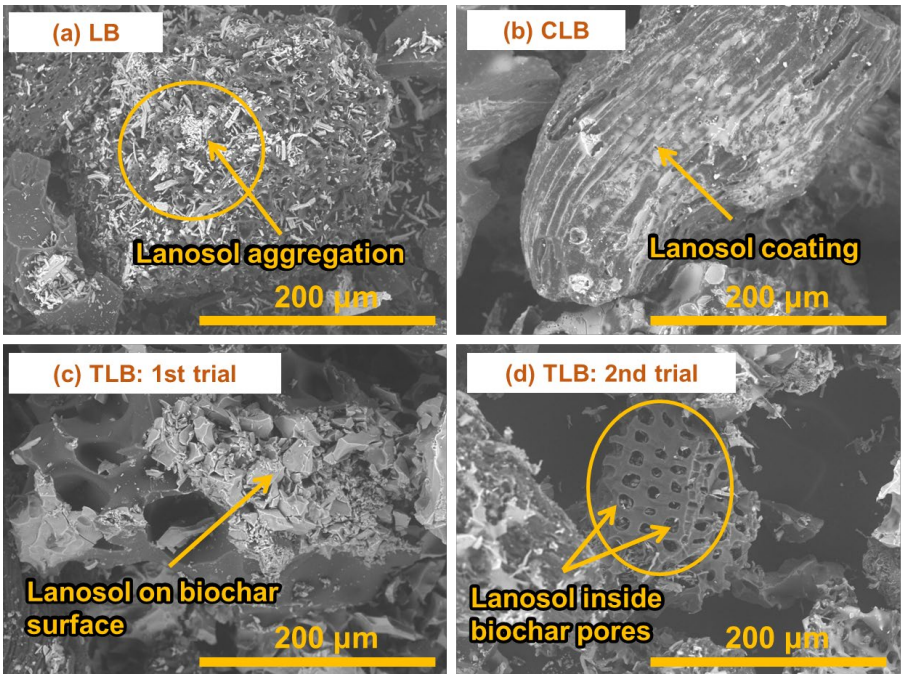

Fig. 2: SEM images of biochar samples after doping with lanosol (LBWG – Dry method doped biochar, CLBWG - Chemically doped biochar, TLBWG – Thermally doped biochar).

1.3 Biocomposites Manufacturing:

For biocomposite manufacturing, WG powder was dry blended with glycerol using an electric mixer for 30 min and then conditioned at room temperature for 12 h. The mixture was flash-frozen in liquid N_2 and ground by a granulator (Retsch GmBH, 5657 HAAN, Germany). The lanosol doped biochar samples were dry blended with the prepared WG powder for 30 min. Additionally, the WG was blended with 4 wt% of lanosol and 4 wt% of biochar, separately, to produce samples for comparison purposes. The loading amount of lanosol and biochar was chosen based on findings in previous work [37, 38]. The final mixtures were compression moulded (or hot pressed) under 250 kN force at 140 °C for 20 min (Fontijne Presses TP 400, Netherlands). The hot pressing temperature was chosen since it was found to be optimal for the processing of WG plastics [39]. The weight fractions of the constituents in samples LBWG, CLBWG, and TLBWG were 65% WG, 25% glycerol, 6% biochar, and 4% lanosol. Table 1 shows the labels of the six samples used in this study.

Table 1: Sample labels

Samples	Labels
Wheat Gluten	WG
Biochar (4 wt.%) + Wheat Gluten	BWG
Lanosol (4 wt.%) + Wheat Gluten	LWG
Dry Mix （Lanosol + Biochar + Wheat Gluten)	LBWG
Chemically Doped（Lanosol + Biochar + Wheat Gluten)	CLBWG
Thermally Doped（Lanosol + Biochar + Wheat Gluten)	TLBWG

1.4 Characterisation:

1.4.1 Mechanical testing:

Biocomposite samples with a width of 12.7 mm, a length of 100 mm, and a thickness of 0.5 mm were tensile tested. An Instron 5566 equipped with a 500 N cell was used to measure tensile modulus (chord modulus between 0.05 and 0.25 % strain), strength, and strain at break based on the ASTM D638 protocol. The crosshead speed and gauge length were 50 mm/min and 50 mm, respectively.

1.4.2 Thermogravimetric analysis (TGA):

Mass loss curves of the blends were obtained by a thermogravimetry analyser (Mettler Toledo TGA/DSC 1 STARe system). The sample in an alumina pan was heated at a constant rate of 10 °C/min from 40 to 750 °C. Furthermore, the derivative (DTG) of mass loss curve was obtained to analyse the decomposition rates. All the samples were tested under nitrogen flow of 50 ml/min [40].

1.4.3 Morphology:

A Hitachi TM 1000 table-top scanning electron microscope (SEM) was employed to analyse the morphology of doped biochar samples and tensile fractured cross sections of composite samples as well as their char residues after the fire test.

1.4.4 Fire testing:

1.4.4.1 Microscale combustion calorimetry:

Combustibility of the samples was measured by a Microscale Combustion Calorimeter (MCC) (Deatak™) using the ASTM D7309 [41]. The thermal degradation (Method A) and thermo-oxidative degradation (Method B) processes were employed for the flammability analysis [15, 42, 43]. The heating rate selected ranged from 0.5 to 5.5 K s^{-1} and the sample mass was 2 mg. For Method A experiments, the samples were pyrolysed in an oxygen free atmosphere from 75 to 600 °C. The volatile effluent was swept out of the pyrolyser using nitrogen gas at a flow rate of 80 cc min^{-1}. Upon entering the combustor, excess oxygen was added to the mixture for a complete oxidation at a temperature of 900 °C. Measurements in Method A are the peak heat release rate (PHRR), total heat release (THR), heat release capacity (HRC), and heat release temperature (pTemp).

With Method B, the samples were heated in an oxidising environment. The end products were pushed out of the specimen chamber by a mixture of nitrogen and oxygen having flow rates of 80

cc min^{-1} and 30 cc min^{-1}, respectively, for combustion in a furnace. Method B provides information on the peak combustion rate (pCR), net calorific value (h_{co}), and the peak combustion temperature (pCT). The samples were labelled according to the names, pyrolysis mode, and heating rates.

1.4.4.2 Cone Calorimetry:

Reaction-to-fire measurements under heat radiation were conducted using a cone calorimeter (FTT Limited, East Grinstead, UK). The biocomposites (100 x 100 mm^2) were tested in a horizontal position by an external heat flux of 50 kW m^{-2}. The distance between the cone heater and sample surface was 25 mm and a balance was equipped to measure mass loss during the testing. In this test, time to ignition (TTI), peak heat release rate (PHRR), and total smoke production (TSP) were addressed to discuss the flammability of the bioplastics. The experiments were in accordance with the processes described in ISO-5660 [44, 45]. All preliminary calibrations were established before the tests were conducted.

1.4.4.3 Statistical analysis:

A single factor analysis of variance (ANOVA) test was performed on the means of the results from the mechanical test. The confidence level was selected as 95% and the Scheffe post hoc test was performed if the null hypothesis was rejected.

2. Results and Discussion:

2.1. Mechanical properties:

Fig. 3a depicts the tensile strength and modulus of the WG bioplastics, whereas Fig. 4 includes all the SEM micrographs of the tensile fractured samples. Neat WG had a semi-brittle fracture, which is observed by the rough surface of the fractured region (Fig. 4a). However, the addition of only lanosol to the WG reduced the tensile strength of the composite by 19 %. A similar observation was made in a previous study [38]. The lanosol particles acted as stress-concentrating points in the WG matrix, nucleating cracks and yielding a lower strength (Fig. 4b). On the other hand, the addition of only biochar to the WG (sample BWG) significantly increased the composite's tensile strength compared to the other samples. This trend was similar to a previously reported study [37]. The tensile strength of the neat WG was 5.4 MPa and the addition of biochar increased it by ca. 19 %. The mechanical interlocking developed between the biochar and WG was attributed to the increase in tensile strength of the composite. The molten WG, during fabrication, infiltrated the empty biochar pores and created an interlaced structure (Fig. 4c). The main reason for the addition of lanosol was to reduce the flammability of the WG. However, because of the higher stress concentration at the lanosol particles, the strength tended to decrease. This deficiency was remedied by the addition of lanosol-doped biochar, however, the blends with lanosol-doped biochar had a variation in properties. The LBWG sample had the lowest tensile strength, statistically similar to the LWG sample, which contained only lanosol. In the LBWG sample, the incomplete doping (see Fig. 3a) resulted in lanosol particles in the WG matrix, which acted as stress concentration points from where the cracks grew (Fig. 4d). Interestingly, the chemically and thermally doped samples (CLBWG and TLBWG) were able to conserve the tensile strength equal to that of the neat WG (their tensile strength values were statistically insignificant). This indicates that the chemical and thermal doping was not detrimental for the strength, which is advantageous where fire behaviour of these composites is concerned (discussed below). Fig.s 4e and 4f depict lanosol particles doped inside biochar pores as well as the mechanical interlocking of the WG matrix and the particle pores. The tensile strengths of these samples (CLBWG and TLBWG) were

lower than that of sample BWG due to the reduced infiltration of molten WG as a result of some of the pores being occupied by lanosol. Nevertheless, this reduction was acceptable because those samples (CLBWG and TLBWG) were able to preserve the tensile strength of the neat WG.

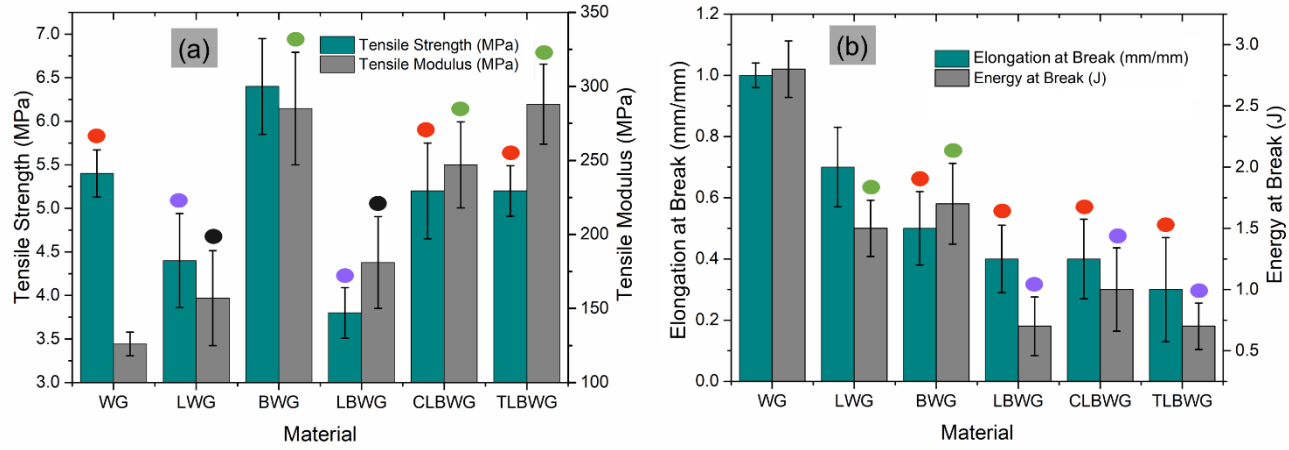

Fig. 3. Tensile properties of WG composites, (a) tensile strength and modulus, (b) Elongation and energy at break (*Results with the same-coloured circle were not significantly different, ANOVA).

The modulus of the neat WG sample was statistically the lowest (Fig. 3a), which was increased by the addition of lanosol, biochar, and lanosol-doped biochar. This result was expected because the addition of these hard particles (compared to the softer polymer) increased the stiffness[20]. The BWG had a maximum modulus of 285 MPa, which was 126 % higher than that of WG. When compared to the WG, the modulus of LBWG, CLBWG, and TLBWG increased by ca. 44, 96, and 111 %, respectively. For tensile strength, the values for CLBWG and TLBWG were statistically lower, but insignificantly different from the modulus of BWG. It is to be noted that for both tensile strength and modulus, the values for LWG and LBWG were statistically insignificant, which shows that the dry mix doping process was inefficient.

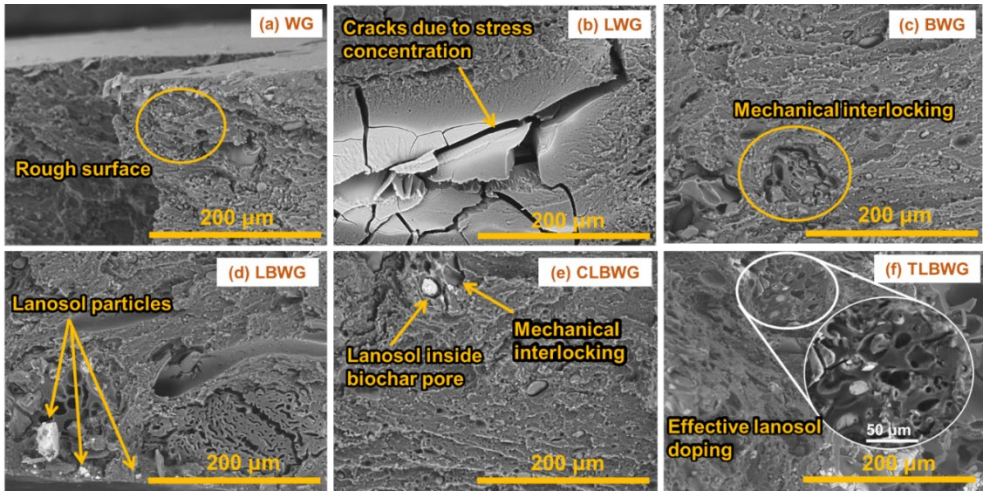

Fig. 4. Fractured surface of tensile tested WG and WG composites.

Fig. 3b shows the Elongation and energy at break of the composite samples. The WG had the highest Elongation at break followed by LWG, BWG, CLBWG, LBWG, and TLBWG. The LWG had a 30% reduction when compared to the WG. The elongation at break of the biochar-added composites (BWG and the lanosol-doped samples) was found to be 50-70 % lower than that of the WG. TLBWG exhibited a maximum reduction of 70%. This was attributed to the brittle nature of the biochar and lanosol particles. The addition of biochar increased the resistance to deformation while decreasing the plasticity. It should be noted that there was no significant difference in the elongation at break between all the biochar-added and lanosol-doped biochar/WG composites. WG had the maximum energy at break of 2.8 J, which was reduced by 40-75 % with only biochar and lanosol-doped biochar addition and 46 % with only lanosol addition (Fig. 3b). The energy at break values of LBWG, CLBWG, and TLBWG were statistically insignificant.

In conclusion, the reinforcement of lanosol-doped biochar did not affect the tensile strength and enhanced modulus compared to neat WG, but it reduced the ductility and toughness. However, it is important to emphasise that the least ductile material, had still a sizeable ductility (an elongation at break of ca. 20 %, Fig. 3b). It is important to note that while FRs, such as lanosol, in polymers, can increase flame resistance, the strength of the resulting composite suffers as a result of stress concentrations caused by the FR particles. However, the current study showed that there is a viable solution to counteract this negative effect. By doping lanosol into biochar, the aforementioned issue can be alleviated, and the polymer's strength and flame resistance can be preserved and increased, respectively. The effect of this doping on the fire and thermal properties of WG composites is discussed in the following sections.

2.2.Flammability Assessment:

2.2.1. Thermogravimetry Analysis (TGA):

The TGA curves shown in Fig. 5a demonstrate a similar mass loss trend for all the samples tested. The initial mass loss (ca. 10 %), which occurred between 100 and 250 °C was mainly attributed to moisture evaporation. The major decomposition that occurred between 250 and 350 °C was due to the disruption of S-S, O-N, and O-O bonds in the peptide along the WG protein chain [46]. Above 450 °C, the composites degraded more slowly until reaching the final temperature of 750 °. The residual mass at 140 °C, 300 °C, and 750 °C were measured and recorded in Table 2. At lower temperatures (140 °C), the mass loss rate was similar for all the samples with the residual mass ranging from 95.2 % to 96.5 %. The LWG and WG samples exhibited the lowest residue content at 300 °C. At 750 °C, the neat WG had the lowest content of residue (16.6 %). The residue increased with the addition of biochar and lanosol depicting the effectiveness of lanosol to enhance the stability over the entire temperature range (higher residue amounts at 750 °C for LBWG, CLBWG and TLBWG compared to the neat WG). Combining the three constituents (i.e., samples LBWG, CLBWG and TLBWG) somewhat lowered the rate of decomposition as compared to the neat WG (Fig.s 5b and c). In other words, the WG sample degraded at a faster rate compared to the other samples. In addition, the peak at the initial stage was more defined in the doped samples (i.e., LBWG, CLBWG and TLBWG) than the un-doped ones (i.e., WG, LWG and BWG). Amongst the lanosol-doped samples, LBWG had the lowest rate of decomposition. This was because of the ineffective doping, which lead to a significant amount of the lanosol particles exposed. Consequently, the higher prevalence of lanosol particles in the matrix conferred somewhat higher stability over the full temperature range than the CLBWG and TLBWG samples.

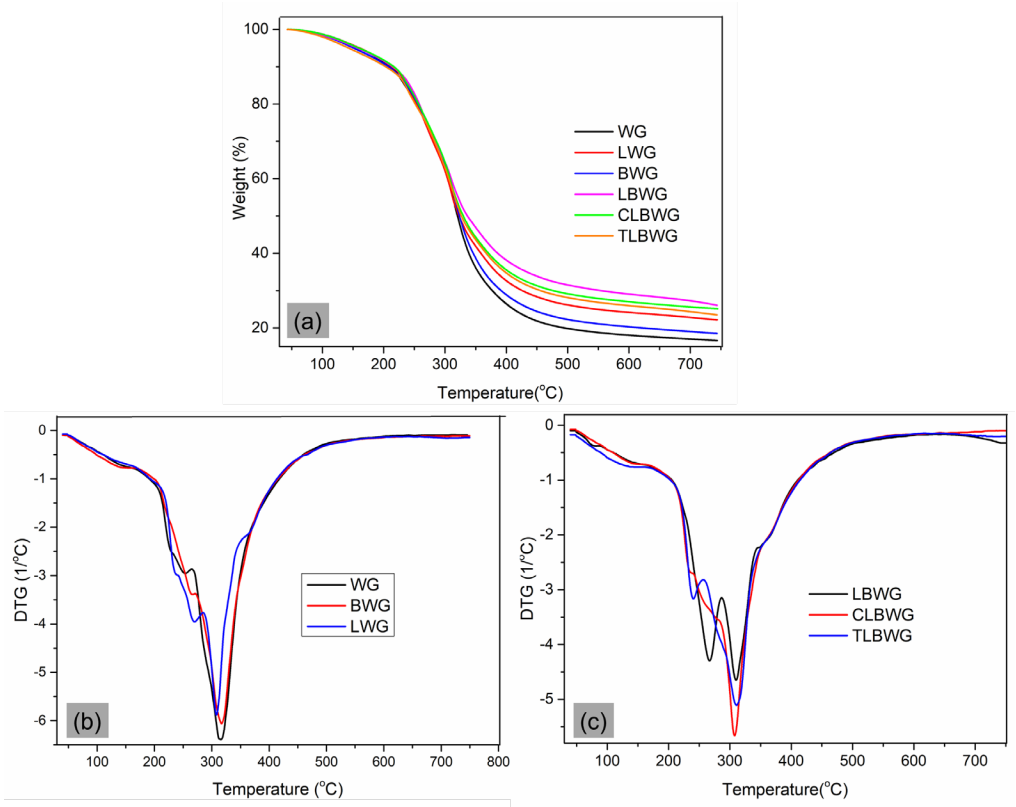

Fig. 5: (a) Mass loss curves of plasticised WG and its composites (b, c), DTG curves of WG and its composites.

Table 2: Residual mass of WG and its composites measured at 140 °C, 300 °C and 750 °C.

Samples	WG	BWG	LWG	LBWG	CLBWG	TLBWG
Weight at 140 °C (%)	96.4	95.9	96.5	96.2	96.4	95.2
300 °C (%)	61.9	63.3	61.7	64.2	64.0	62.7
750 °C (%)	16.6	18.5	22.2	26.1	25.2	23.5

2.2.2. Microscale Combustion Calorimeter Results:

The heat release parameters of the samples obtained with Methods A and B modes of MCC are discussed in this section. Table 3 lists the averages of experimental results from 0.5 to 5.5 K s^{-1} heating rates. Due to the large variation of PHRR and pCR, these exhibited also the highest standard deviations. Characteristic graphs showing the HRR curves at these heating rates are also presented in Fig. S1 (Supplementary information). It is evident from Table 3 that the addition of lanosol (sample LWG) and biochar (sample BWG) to WG reduced its flammability, and the effect was highest with lanosol. The addition of lanosol yielded a drastic reduction (ca. 30 %) in both PHRR and pCR. HRC was reduced by 31 %, while THR attained a 30 % decrease. Lanosol is a flame retardant, thus it improves the fire performance of plastics by reducing the PHRR. At the same heating rates, it was seen that the combustion temperature increased, although the net calorific value and pTemp both decreased (Table 3). A slight improvement in the flame retardancy

performance was observed when biochar was mixed with the WG powder (BWG). The peak heat release temperature was higher (371 °C) compared to that of LWG (354 °C). The combined effects of lanosol and biochar on WG (LBWG) are also clearly shown. As seen in the plots in Fig. S1, the HRR curves have three distinct peaks indicating the degradation of the respective compositions. Expectedly, the flame retardancy performance of LBWG was a balance between that of the separate mixtures of LWG and BWG (Table 3). Considering the doped samples, CLBWG had somewhat better heat release properties than TLBWG (Table 3). Both methods produced similar results and the differences were almost insignificant. The particularly outstanding parameter was the pCT of the chemically doped composite (450 °C), which was significantly higher than that of the thermally doped sample (375 °C). In general, the doping lowered the PHRR for the neat WG, with the strongest effect shown for the LBWG sample, although the differences between the doped samples were not significant. Nevertheless, it can be concluded that the addition of lanosol-doped biochar to WG, lowered its PHRR, HRC, and pCR, indicating higher fire-resistance of the doped samples.

Table 3: Average values of heat release parameters measured by MCC

Samples	Method A				Method B			
	PHRR (W g^{-1})	**pTemp (°C)**	**HRC (J g^{-1} K^{-1})**	**THR (kJ g^{-1})**	**pCR (W g^{-1})**	**pCT (°C)**	**HRC (J g^{-1} K^{-1})**	**h_c^o (kJ g^{-1})**
WG	336±175	374±27	120±22	20±7	300±178	367±32	99±9.1	13±2
LWG	239±123.8	354±24	83±10	14±3	212±119.5	379±71	78±12.5	15±4
BWG	330±160	371±22	116±13	17±3	279±140	347±24	89±8.7	14±2
LBWG	272±130.7	348±23	98±16	14±4	219±119	367±25	86±14.8	16±3
CLBWG	284±138.4	350±16	97±12	17±3	235±121.6	450±19	75±22.6	15±3
TLBWG	289±144	344±18	100±13	16±3	243±137.2	375±17	79±24	16±4

2.2.2.1. The effect of lanosol and biochar on the ignition temperature (T_{ign}) of WG:
Pyrolysis generates volatile fuel fragments which escape to the gas phase and mix with oxygen or air. The minimum temperature required to initiate combustion of the combustible mixture is the ignition temperature. The ability of a material to resist flaming combustion is characterised by the time and temperature of ignition. Hence, the higher the ignition temperature, the lower is the flammability of the material. The temperature corresponding to 5 % of the integrated HRR versus temperature curve was recorded as T_{ign}. The T_{ign} values of the WG and its composites are shown in Tables S1 to S3 as well as in Fig. 6. Since there is a peak at the initial pyrolysis stage of the thermal decomposition process, the ignition temperatures in Method B were higher than in Method A. According to the results, the average ignition temperature at 0.5 to 5.5 Ks^{-1} heating rate for neat WG was 130 and 238 °C, respectively, for Methods A and B. The addition of lanosol to WG resulted in a decrease in T_{ign} to 110 °C in Method A. However, due to the presence of excess oxygen in Method B, the reaction of bromine gas was delayed, thereby extending the ignition to higher temperatures [47]. This is demonstrated with an increase of T_{ign} to 250 °C for the thermal

oxidative decomposition process. The BWG sample somewhat maintained the ignition temperatures of the neat WG. The T_{ign} for the LBWG was lower while the CLBWG and TLBWG samples showed no increase. It is worth noting that the thermally doped composite (TLBWG) showed the highest ignition temperature (Method B) amongst all the samples tested which could be attributed to the effective doping of lanosol and biochar, although the difference was not statistically significant.

2.2.2.2.The effect of lanosol and biochar on the Ignition Capacity (IGC) of WG:

The ignition capacity (IGC) shows a material's propensity to ignite when exposed to adequate thermal energy. It is defined as the ratio of heat released during the entire combustion process to the ignition temperature. For any material, the lower the IGC is, the better is the flame resistance. The ignition capacity of the composites and neat WG using Methods A and B are shown in Table S1 – Table S3 and Fig. 6. A relatively high IGC (152 J g^{-1} K^{-1}) was obtained for neat WG in Method A. Interestingly, lanosol and biochar greatly lowered the IGC value of the WG. The LWG and BWG samples had an IGC of 132.1 and 110.4 J g^{-1} K^{-1}, respectively. The IGC of the thermally doped sample (TLBWG) was 125.8 J g^{-1} K^{-1}. However, the chemically doped samples (CLBWG) attained an IGC of 142.1 J g^{-1} K^{-1}. On the other hand, Method B yielded results with a different trend. The neat WG had the least IGC, followed by LWG, then the CLBWG, BWG, and TLBWG. The order may have been influenced by the oxidative pyrolysis mode. From a general point of view, the samples tested with Method A had higher IGCs than the Method B samples. Nevertheless, considering Method A, the thermally doped sample reduced the IGC of the composite compared to the neat WG, which is an advantageous trait.

2.2.2.3. The effect of lanosol and biochar on the Fire Growth Capacity (FGC) of WG:

A material's potential for fire growth by ignition and flame spread is known as fire growth capacity (FGC). FGC combines the ability of a material to ignite with or without an ignition source (IGC) and its propensity to release heat is referred to as HRC, which is used to estimate the rate of fire growth. In flammability analysis, FGC values of materials are compared to ascertain their similarities with respect to flammability. Lower FGC values signify better ignition and flame resistance. It can also be estimated by using Equation 1 [48].

$$FGC = \left(\frac{Q_\infty}{T_2 - T_1}\right)\left(\frac{T_2 - T_0}{T_1 - T_0}\right) \qquad (1)$$

where Q_∞ is the total heat release, T_0 is the ambient temperature, which is 25 °C, T_1 is the ignition temperature and the burn out temperature is T_2. The FGC results for WG composites are presented in Fig. 6 as well as in Tables S1 – S3. The FGC results for Method A followed a similar pattern as the IGC data. FGC of WG saw a sharp decrease with the addition of lanosol (LWG) while biochar (BWG) decreased it by only 25 J g^{-1} K^{-1}. Among the samples with three combined components, CLBWG had the highest FGC, with LBWG showing a relatively low FGC value (212 J g^{-1} K^{-1}), while the FGC of the TLBWG sample lying between the two aforementioned samples. Considering the results from Method B, the CLBWG and LWG composites had lower FGC; 135 J g^{-1} K^{-1} and 137 J g^{-1} K^{-1}, respectively, compared to the WG sample. These samples (CLBWG and LWG) were able to resist fire growth due to the presence of lanosol coating on the surface of the composites (Fig.2).

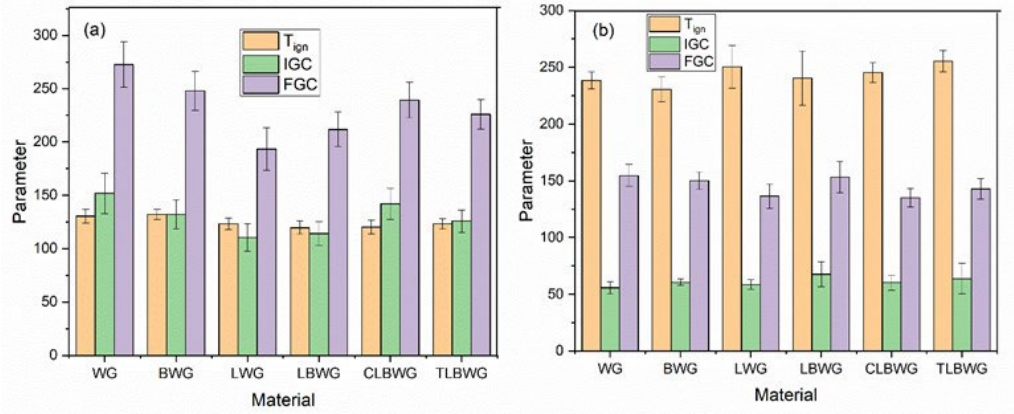

Fig. 6: T_{ign}, IGC and FGC of WG composites (a) Method A and (b) Method B.

2.2.2.4.Estimation of the activation energy (E_a) of WG composites:

The activation energy represents the minimum amount of energy required to initiate decomposition reactions. It can be used to predict material properties, such as HRC [49]. In this study, the Kissinger equation, defined in ASTM E698-05, was applied in the estimation of the average activation energy. With the Kissinger method, the peak heat release or combustion temperature obtained at each heating rate applied were considered as constant conversion points. The Kissinger equation is shown in Equation 2 [50]. Plotting $\ln\left[\frac{\beta}{T_p^2}\right]$ against $\left[\frac{1}{T_p}\right]$ yields a straight line with the slope being $\left[\frac{-E_a}{R}\right]$. E_a can thus be calculated from the slope:

$$\ln\left[\frac{\beta}{T_p^2}\right] = \ln\left[\frac{AR}{E_a}\right] - \frac{E_a}{RT_p} \qquad (2)$$

where β is the heating rate, R is the gas constant, A is the pre-exponential factor, and $T_{p,}$ the average of the peak heat release temperature (pTemp) in Table 3. Fig.s S2a and S2b show the plots used to estimate the activation energies for Method A and Method B, respectively. Table 4 shows the E_a values with the corresponding statistical indices depicting the accuracy of the results. Since the average values of pTemp were used for the estimation, the standard deviation of the E_a values was omitted in the table (but provided in Fig. 7). Fig. 7 compares the activation energies obtained with the Method A and B experimental procedures. The Kissinger method does not capture the change in E_a for the entire pyrolysis process, hence, the activation energy here is referred to as an apparent activation energy. The activation energy of the WG pyrolysis reaction was 24.2 kJ mol^{-1}, which was the same when lanosol (LWG) was added. The addition of biochar (BWG) yielded a slower reaction, requiring a higher activation energy (32.5 kJ mol^{-1}). The combination of lanosol and biochar in WG (LBWG) tended to decrease the activation energy, however, the doping process, especially the thermal doping (TLBWG), increased the activation energy. The results from the thermal oxidative decomposition were similar to that of Method A although lower E_a values were recorded (14.4 - 19 kJ mol^{-1}) as shown in Table 4 and Fig. 7. Additionally, it was observed that the R-value for WG was higher than the composites, which could mean that the addition of flame retardants and the manufacturing process affected the accuracy of the estimations (Table 4). This analysis proves that the effective doping of WG with lanosol and biochar increased

the minimum amount of energy required by WG for a burning reaction to take place thereby delaying the burning rate of WG.

Table 4: Activation energy values of WG and its composites

Samples	Method A			Method B		
	E_a/kJ mol^{-1}	Pearson's R	Standard error	E_a/kJ mol^{-1}	Pearson's R	Standard error
WG	24.2	0.99	0.24	19.0	0.96	0.64
LWG	24.2	0.91	1.31	16.2	0.75	1.73
BWG	32.5	0.98	0.65	18.1	0.71	2.18
LBWG	22.7	0.75	2.42	14.4	0.84	0.84
CLBWG	29.2	0.91	1.65	15.8	0.93	0.63
TLBWG	32.4	0.90	1.81	16.8	0.85	1.69

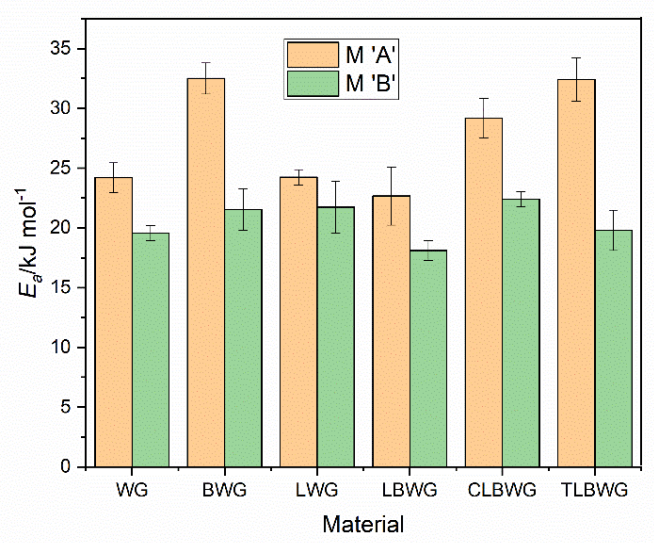

Fig. 7: Comparison of activation energies calculated from Method A (M 'A') and B (M'B') results.

2.3.Cone Calorimeter Results:

The peak heat release rate (PHRR), time to ignition (TTI), time to PHRR (TTPHRR), total smoke production (TSP), THR for neat WG, and the composites were measured with a cone calorimeter. The average results of two tested samples are summarised in Table 5. The fire performance index (FPI) and fire growth index (FGI), representing the response of the material to a radiation heat source, were estimated from PHRR, TTI, and TPHRR. Illustrations of the heat release rate curves for the materials are also displayed in Fig. 8. The shapes of the HRR curves are similar, except for the thermally doped sample (TLBWG), which showed a small shoulder before the main peak. The BWG sample had the highest PHRR (694 kW m^{-2}), which was unexpected because the high temperature biochar used is a fire-resistant carbon skeleton hence, it should have a flame retardant effect on the WG. The lowest PHRR was recorded for TLBWG. The cone test results presented a clear distinction between the heat release and ignition parameters of the chemical and thermal

doping techniques. The results in Table 5 indicated that the TLBWG sample was more fire resistant compared to the CLBWG sample.

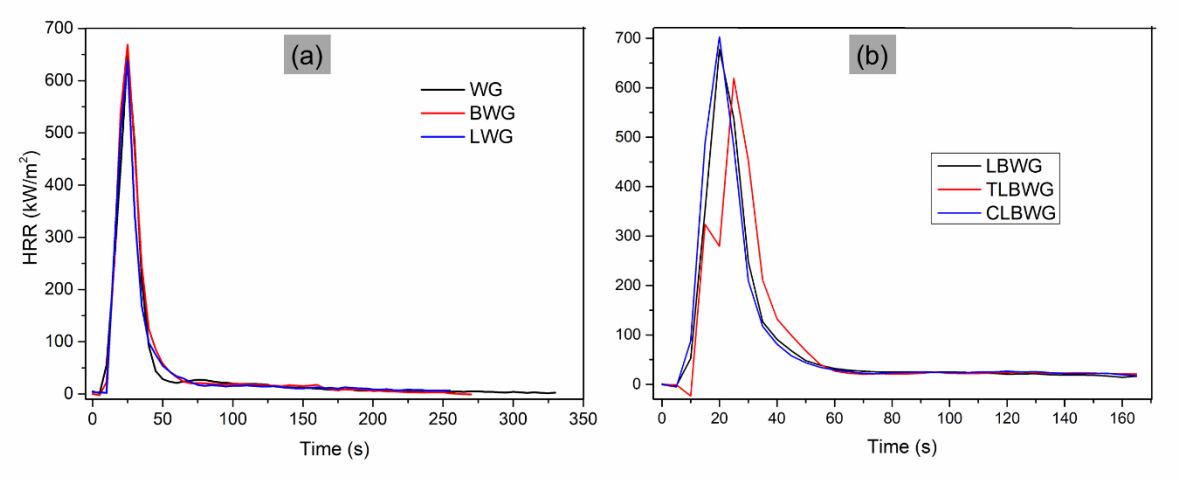

Fig. 8: Cone calorimeter analysis of the WG samples.

The total smoke produced in table 5 is lower for WG than the other samples due to the higher amount of smoke released during smouldering or charring of materials. This further confirms the flame retardant mechanism of the doped fire retardant. The ratio of TSP to total heat released (TSP/THR) is used to distinguish between materials that release more or less smoke than heat in the burning process. The results listed in Table 5 indicate that TLBWG showed the highest TSP/THR (0.096 m^2 MJ^{-1}), which also confirmed that although the TLBWG composite produced the lowest amount of heat, the quantity of generated smoke was the highest. This is one of the issues to consider when producing TLBWG materials on a large scale. The char residue from the cone test experiments of TLBWG and CLBWG are shown in Fig. 9. Similar quantities of char residues were obtained from the tests. The SEM images show a dense residue structure with small holes for TLBWG while a rugged and cracked char is observed in that of CLBWG. The dense char residue shielded the underlying virgin material from the ambient O_2 causing incomplete combustion in these samples, thereby increasing the amount of smoke produced. The effective lanosol doping in TLBWG preserved the structural integrity and reduced the effect of the heat exposure on the material.

Table 5: Cone calorimetry results of WG composites

Samples	PHRR (kW m^{-2})	TTPHRR	TTI (s)	THR (MJ m^{-2})	TSP (m^2)	TSP/THR (m^2 $(MJ)^{-1}$)
WG	652±38	25±15	23.0±4.0	13.1±7.0	0.6±0.0	0.046±0.0
BWG	694±94	25±0	12.5±0.7	13.4±0.2	0.6±0.0	0.045±0.0
LWG	645±10	25±0	14±4.0	11.8±0.3	1.1±0.1	0.089±0.08
LBWG	648±41	20±0	11.5±0.7	12±0.4	1.0±0.0	0.084±0.0
CLBWG	686±24	20±0	10.5±0.7	11.7±0.07	1.0±0.1	0.086±0.08
TLBWG	636±24	22.5±3.5	13±2.8	11.5±1.3	1.1±0.0	0.096±0.01

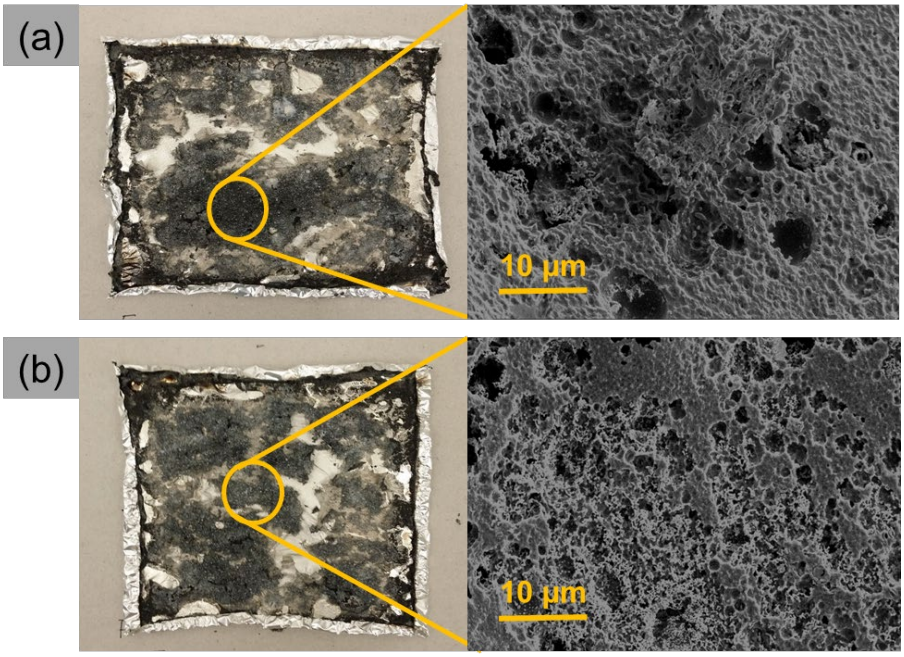

Fig. 9: Cone calorimeter post-test char residue (a) CLWBG and (b) TLWBG.

3. Conclusions:

In this study, the effects of lanosol-doped biochar on the mechanical and fire properties of a WG bioplastic were investigated. To make the WG composites, 4 wt.% lanosol was doped into 6 wt.% biochar using mechanical (dry mixing), chemical, and thermal doping techniques. The results showed that the new approach for improving the fire-resistant properties of protein-based bioplastics was successful in that it preserved the mechanical strength. The thermal and chemical doping techniques were found to be the most effective in placing significant amount of lanosol inside the biochar pores. The addition of only biochar to the bioplastic increased the tensile strength and modulus the most. However, the thermally and chemically lanosol-doped biochar composites were able to retain the strength of the neat WG bioplastic with a higher modulus. On the other hand, the addition of doped biochar to WG reduced its ductility, which was expected. However, the material was still quite ductile.

The TGA analysis of the samples showed a higher residue and slower decomposition rates for the doped samples compared to the neat WG, thus, the stability of the WG, over the full temperature range, was enhanced after doping. Additionally, from the MCC experiments, it was observed that the doped samples had lower peak heat release rate, peak combustion rate, heat release and ignition capacities than the neat WG, indicating an improvement in flame resistance. In general, all the doping methods reduced the peak heat release rates of neat WG with the thermally doped sample exhibiting the lowest value according to the cone test. Moreover, the structural integrity of the char residue, in the thermally doped sample, was preserved after the cone calorimeter test, confirming the effectiveness of the doping process. The same sample had the highest activation energy and the lowest ignition and fire growth capacities. Hence, based on the results of the various tests, it can be concluded that thermally doping lanosol into biochar is the most feasible method to impart fire retardancy and retain mechanical strength in protein-based bioplastics. Additional studies should be carried out to optimise the doping method. The new approach is probably useful (and generic) in other polymer systems, but additional work must be made to confirm this.

References

[1] W.-Q. Yuan, H. Zhang, Y.-X. Weng, Y.-D. Li, J.-B. Zeng, Fully biobased polylactide/epoxidized soybean oil resin blends with balanced stiffness and toughness by dynamic vulcanization, Polymer Testing, 78 (2019) 105981.
[2] H.V. Ford, N.H. Jones, A.J. Davies, B.J. Godley, J.R. Jambeck, I.E. Napper, C.C. Suckling, G.J. Williams, L.C. Woodall, H.J. Koldewey, The fundamental links between climate change and marine plastic pollution, Science of The Total Environment, 806 (2022) 150392.
[3] R.A. Mensah, V. Shanmugam, S. Narayanan, J.S. Renner, K. Babu, R.E. Neisiany, M. Försth, G. Sas, O. Das, A review of sustainable and environment-friendly flame retardants used in plastics, Polymer Testing, 108 (2022) 107511.
[4] N.F. Attia, A.M. Eid, M.A. Soliman, M. Nagy, Exfoliation and Decoration of Graphene Sheets with Silver Nanoparticles and Their Antibacterial Properties, Journal of Polymers and the Environment, 26 (2018) 1072-1077.
[5] O. Das, T.A. Loho, A.J. Capezza, I. Lemrhari, M.S. Hedenqvist, A novel way of adhering PET onto protein (wheat gluten) plastics to impart water resistance, Coatings, 8 (2018) 388.
[6] X.-Z. Wang, J. He, Y.-X. Weng, J.-B. Zeng, Y.-D. Li, Structure-property relationship in fully biobased epoxidized soybean oil thermosets cured by dicarboxyl terminated polyamide 1010 oligomer with different carboxyl/epoxy ratios, Polymer Testing, 79 (2019) 106057.
[7] D. Taufik, M.J. Reinders, K. Molenveld, M.C. Onwezen, The paradox between the environmental appeal of bio-based plastic packaging for consumers and their disposal behaviour, Science of The Total Environment, 705 (2020) 135820.
[8] J.M. Farias da Silva, B.G. Soares, Epoxidized cardanol-based prepolymer as promising biobased compatibilizing agent for PLA/PBAT blends, Polymer Testing, 93 (2021) 106889.
[9] R. Sharma, O. Das, S.G. Damle, A.K. Sharma, Isocitrate lyase: a potential target for anti-tubercular drugs, Recent Patents on Inflammation & Allergy Drug Discovery, 7 (2013) 114-123.
[10] O. Das, D. Bhattacharyya, Development of polymeric biocomposites: particulate incorporation, interphase generation and evaluation by nanoindentation, Interface/interphase in polymer nanocomposites, (2016) 333-374.
[11] I.S. Santos, B.L. Nascimento, R.H. Marino, E.M. Sussuchi, M.P. Matos, S. Griza, Influence of drying heat treatments on the mechanical behavior and physico-chemical properties of mycelial biocomposite, Composites Part B: Engineering, 217 (2021) 108870.
[12] F. Chegdani, M. El Mansori, A.-A. Chebbi, Cutting behavior of flax fibers as reinforcement of biocomposite structures involving multiscale hygrometric shear, Composites Part B: Engineering, 211 (2021) 108660.
[13] A. Aminoroaya, R.E. Neisiany, S.N. Khorasani, P. Panahi, O. Das, H. Madry, M. Cucchiarini, S. Ramakrishna, A review of dental composites: Challenges, chemistry aspects, filler influences, and future insights, Composites Part B: Engineering, 216 (2021) 108852.
[14] S. Vigneshwaran, R. Sundarakannan, K.M. John, R.D.J. Johnson, K.A. Prasath, S. Ajith, V. Arumugaprabu, M. Uthayakumar, Recent advancement in the natural fiber polymer composites: A comprehensive review, Journal of Cleaner Production, (2020) 124109.
[15] R. Afriyie Mensah, J. Xiao, O. Das, L. Jiang, Q. Xu, M. Okoe Alhassan, Application of Adaptive Neuro-Fuzzy Inference System in Flammability Parameter Prediction, Polymers, 12 (2020) 122.
[16] Z. Yang, H. Li, G. Niu, J. Wang, D. Zhu, Poly(vinylalcohol)/chitosan-based high-strength, fire-retardant and smoke-suppressant composite aerogels incorporating aluminum species via freeze drying, Composites Part B: Engineering, 219 (2021) 108919.

[17] K. Sykam, M. Försth, G. Sas, A. Restas, O. Das, Phytic acid: A bio-based flame retardant for cotton and wool fabrics, Industrial Crops and Products, 164 (2021) 113349.
[18] A. Veerasimman, V. Shanmugam, S. Rajendran, D.J. Johnson, A. Subbiah, J. Koilpichai, U. Marimuthu, Thermal Properties of Natural Fiber Sisal Based Hybrid Composites–A Brief Review, Journal of Natural Fibers, (2021) 1-11.
[19] S. Mohan Bhasney, A. Kumar, V. Katiyar, Microcrystalline cellulose, polylactic acid and polypropylene biocomposites and its morphological, mechanical, thermal and rheological properties, Composites Part B: Engineering, 184 (2020) 107717.
[20] O. Das, D. Bhattacharyya, D. Hui, K.-T. Lau, Mechanical and flammability characterisations of biochar/polypropylene biocomposites, Composites Part B: Engineering, 106 (2016) 120-128.
[21] O. Das, N.K. Kim, A.L. Kalamkarov, A.K. Sarmah, D. Bhattacharyya, Biochar to the rescue: Balancing the fire performance and mechanical properties of polypropylene composites, Polymer degradation and stability, 144 (2017) 485-496.
[22] Y.N. Kim, Y.-M. Ha, J.E. Park, Y.-O. Kim, J.Y. Jo, H. Han, D.C. Lee, J. Kim, Y.C. Jung, Flame retardant, antimicrobial, and mechanical properties of multifunctional polyurethane nanofibers containing tannic acid-coated reduced graphene oxide, Polymer Testing, 93 (2021) 107006.
[23] X. Wang, J. Sun, X. Liu, S. Jiang, J. Wang, H. Li, S. Bourbigot, X. Gu, S. Zhang, An effective flame retardant containing hypophosphorous acid for poly (lactic acid): Fire performance, thermal stability and mechanical properties, Polymer Testing, 78 (2019) 105940.
[24] N.F. Attia, B.K. Saleh, Novel synthesis of renewable and green flame-retardant, antibacterial and reinforcement material for styrene–butadiene rubber nanocomposites, Journal of Thermal Analysis and Calorimetry, 139 (2020) 1817-1827.
[25] K. Babu, O. Das, V. Shanmugam, R.A. Mensah, M. Försth, G. Sas, Á. Restás, F. Berto, Fire Behavior of 3D-Printed Polymeric Composites, Journal of Materials Engineering and Performance, 30 (2021) 4745-4755.
[26] C.M. Tai, R.K.Y. Li, Mechanical properties of flame retardant filled polypropylene composites, Journal of applied polymer science, 80 (2001) 2718-2728.
[27] N. Attia, H. Ahmed, D. Yehia, M. Hassan, Y. Zaddin, Novel synthesis of nanoparticles-based back coating flame-retardant materials for historic textile fabrics conservation, Journal of Industrial Textiles, 46 (2017) 1379-1392.
[28] N.F. Attia, S.E.A. Elashery, A.M. Zakria, A.S. Eltaweil, H. Oh, Recent advances in graphene sheets as new generation of flame retardant materials, Materials Science and Engineering: B, 274 (2021) 115460.
[29] D.C.C.d.S. Medeiros, C. Nzediegwu, C. Benally, S.A. Messele, J.-H. Kwak, M.A. Naeth, Y.S. Ok, S.X. Chang, M. Gamal El-Din, Pristine and engineered biochar for the removal of contaminants co-existing in several types of industrial wastewaters: A critical review, Science of The Total Environment, (2021) 151120.
[30] B.O. Nardis, J.R. Franca, J.S.d.S. Carneiro, J.R. Soares, L.R.G. Guilherme, C.A. Silva, L.C.A. Melo, Production of engineered-biochar under different pyrolysis conditions for phosphorus removal from aqueous solution, Science of The Total Environment, (2021) 151559.
[31] Y. Wu, C. Brickler, S. Li, G. Chen, Synthesis of microwave-mediated biochar-hydrogel composites for enhanced water absorbency and nitrogen release, Polymer Testing, 93 (2021) 106996.
[32] O. Das, A.K. Sarmah, D. Bhattacharyya, Structure–mechanics property relationship of waste derived biochars, Science of The Total Environment, 538 (2015) 611-620.

[33] D.M. Paleri, A. Rodriguez-Uribe, M. Misra, A.K. Mohanty, Pyrolyzed biomass from corn ethanol industry coproduct and their polypropylene-based composites: Effect of heat treatment temperature on performance of the biocomposites, Composites Part B: Engineering, 215 (2021) 108714.
[34] K. Aup-Ngoen, M. Noipitak, Effect of carbon-rich biochar on mechanical properties of PLA-biochar composites, Sustainable Chemistry and Pharmacy, 15 (2020) 100204.
[35] O. Das, R.E. Neisiany, A.J. Capezza, M.S. Hedenqvist, M. Försth, Q. Xu, L. Jiang, D. Ji, S. Ramakrishna, The need for fully bio-based facemasks to counter coronavirus outbreaks: A perspective, Science of The Total Environment, 736 (2020) 139611.
[36] N.F. Attia, Organic nanoparticles as promising flame retardant materials for thermoplastic polymers, Journal of Thermal Analysis and Calorimetry, 127 (2017) 2273-2282.
[37] O. Das, M.S. Hedenqvist, E. Johansson, R.T. Olsson, T.A. Loho, A.J. Capezza, R.K. Singh Raman, S. Holder, An all-gluten biocomposite: Comparisons with carbon black and pine char composites, Composites Part A: Applied Science and Manufacturing, 120 (2019) 42-48.
[38] O. Das, N.K. Kim, M.S. Hedenqvist, D. Bhattacharyya, E. Johansson, Q. Xu, S. Holder, Naturally-occurring bromophenol to develop fire retardant gluten biopolymers, Journal of Cleaner Production, 243 (2020) 118552.
[39] Q. Wu, S. Yu, M. Kollert, M. Mtimet, S.V. Roth, U.W. Gedde, E. Johansson, R.T. Olsson, M.S. Hedenqvist, Highly absorbing antimicrobial biofoams based on wheat gluten and its biohybrids, ACS Sustainable chemistry & engineering, 4 (2016) 2395-2404.
[40] N.F. Attia, M. Mousa, Synthesis of smart coating for furniture textile and their flammability and hydrophobic properties, Progress in Organic Coatings, 110 (2017) 204-209.
[41] V. Benin, S. Durganala, A.B. Morgan, Synthesis and flame retardant testing of new boronated and phosphonated aromatic compounds, Journal of Materials Chemistry, 22 (2012) 1180-1190.
[42] R.A. Mensah, L. Jiang, S. Asante-Okyere, Q. Xu, C. Jin, Comparative evaluation of the predictability of neural network methods on the flammability characteristics of extruded polystyrene from microscale combustion calorimetry, Journal of Thermal Analysis and Calorimetry, 138 (2019) 3055-3064.
[43] R.A. Mensah, Q. Xu, S. Asante-Okyere, C. Jin, G. Bentum-Micah, Correlation analysis of cone calorimetry and microscale combustion calorimetry experiments, Journal of Thermal Analysis and Calorimetry, 136 (2019) 589-599.
[44] I.S.O.R.-t.-F. Tests-Heat, Release, Smoke Production and Mass Loss Rate-Part 1: Heat Release Rate (Cone Calorimeter Method) and Smoke Production Rate (Dynamic Measurement), International Organization for Standardization: Geneva, Switzerland, (2015) 5660.
[45] N.F. Attia, E.M. Hegazi, A.A. Abdelmageed, Smart modification of inorganic fibers and flammability mechanical and radiation shielding properties of their rubber composites, Journal of Thermal Analysis and Calorimetry, 132 (2018) 1567-1578.
[46] O. Das, A.K. Sarmah, D. Bhattacharyya, Biocomposites from waste derived biochars: Mechanical, thermal, chemical, and morphological properties, Waste management, 49 (2016) 560-570.
[47] G.B. Heisig, H.M. Davis, The Effect of Oxygen on the Reaction between Bromine and Butadiene, Journal of the American Chemical Society, 58 (1936) 1095-1097.
[48] J.G. Quintiere, Fire growth: an overview, Fire technology, 33 (1997) 7-31.
[49] Q. Xu, C. Jin, A. Majlingova, A. Restas, Discuss the heat release capacity of polymer derived from microscale combustion calorimeter, Journal of Thermal Analysis and Calorimetry, 133 (2018) 649-657.

[50] C. Jia, J. Chen, J. Liang, S. Song, K. Liu, A. Jiang, Q. Wang, Pyrolysis characteristics and kinetic analysis of rice husk, Journal of Thermal Analysis and Calorimetry, 139 (2020) 577-587.

Part 2: Investigation of the most suitable FR, bioplastic and the processing method

1. Experimental:

1.1. Materials:

In this part of the project, the doping method selected was thermal (i.e. TLBWG) but along with WG, APP was also doped in the biochar. However, when doping the APP, the temperature used was 230 ℃ instead of 135 ℃, which was for lanosol. This is based on the melting points of the respective FRs. The WG used was the same as explained in Part 1 of this report in section 1.1. The PA 11 was obtained from Arkema (France) in powder form. The APP was procured from Sigma Aldrich, Sweden.

1.2. Experimental design:

The experiments in this part of the project were designed in order to identify the most suitable FR, bioplastic and processing technique, from the sets of two selected for the entire investigation. The selection was done in an incremental manner wherein first the most suitable FR was identified followed by the bioplastic and the processing method, as shown in Fig. 1. For lanosol, the weight percentage of biochar was 6 and that of lanosol was 4. In the same line, for APP, the weight percentage of biochar was 22.5 whereas the same was 15 for APP. The optimal amount of APP in a polymeric system varies from 15 – 30 wt% [1]. The rest was the respective polymer (WG or PA 11). Note that WG was plasticised with 25 % glycerol as plasticiser.

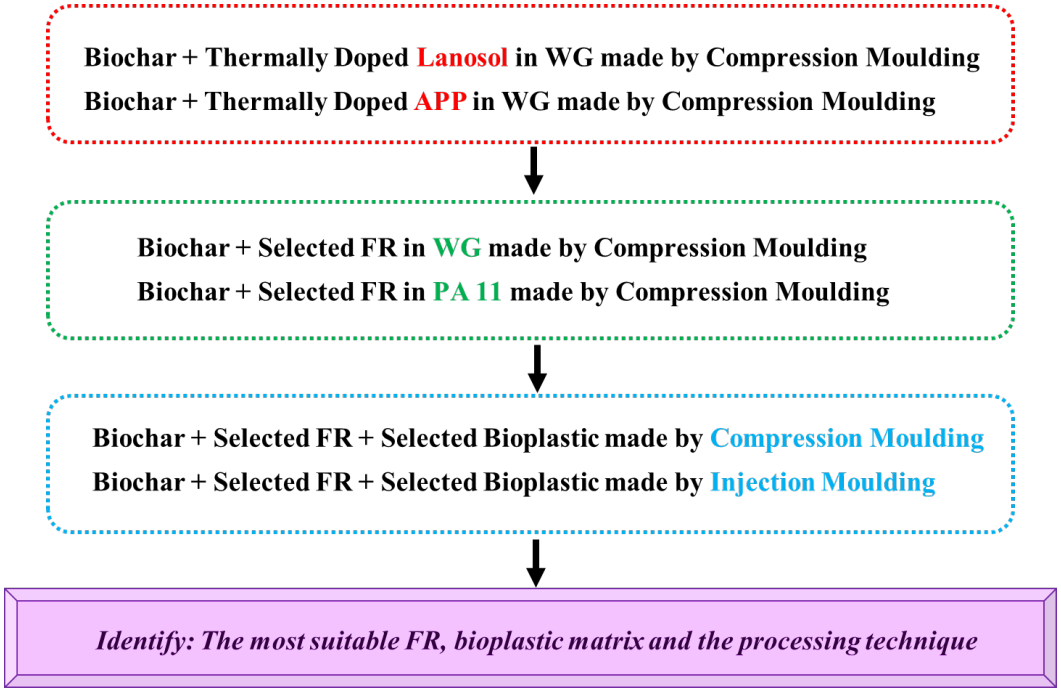

Fig. 1. Experimental design

The samples were named accordingly:

- Neat wheat gluten: Neat WG
- Neat polyamide 11: Neat PA 11

- Biochar with thermally doped lanosol in WG made by compression moulding: BC_Lanosol_WG_COMP
- Biochar with thermally doped APP in WG made by compression moulding: BC_APP_WG_COMP
- Biochar with thermally doped APP in WG made by injection moulding: BC_APP_WG_INj
- Biochar with thermally doped APP in PA 11 made by compression moulding: BC_APP_PA11_COMP

1.3. Processing:

The manufacturing of the samples was done by mixing the constituents (bioplastic, FR-doped biochar and plasticiser) through dry blending followed by flash freezing in liquid N_2 and grinding (Retsch GmBH, 5657 HAAN, Germany). Note that PA 11 did not require the use of a plasticiser or flash freezing. Instead, the samples with PA 11 were directly dry blended and subjected to processing. The samples were compression moulded (Fortijne Presses TP 400, Netherlands). The processing conditions for the compression moulding were decided from trial runs, which caused a desirable sample finish. For WG-based samples, the pressing temperature was 140 °C; force: 250 kN; pressing time = 20 min. For PA 11-based samples, the pressing temperature was 250 °C; force: 250 kN; pressing time = 20 min. The mould used yielded sheets with the dimension: 100 • 100 • 4 $(mm)^3$. For injection moulding (Thermofisher), the sample mix powders (only WG-based) were subjected to various injection time of 3, 5, 15 and 20 s and the temperature was 140 °C with an injection pressure of 600 psi. Fig. 2 shows the summary of the processing conditions.

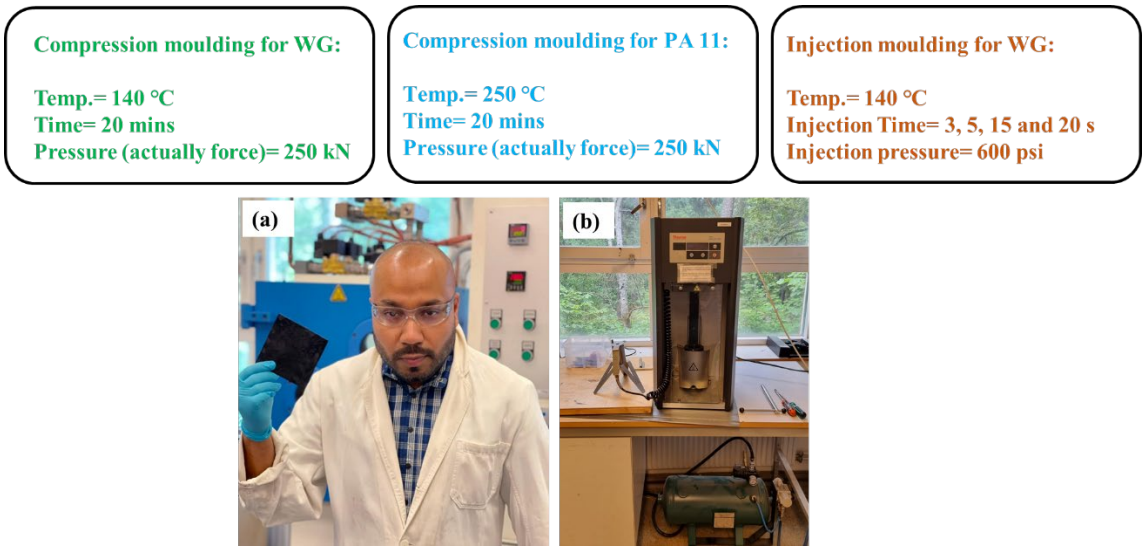

Fig. 2. A summary of the processing conditions used for the part 2 of the project. a) Oisik Das holding a compression mounded sample with the instrument in the background, b) the injection moulding machine used in the project.

1.4. Characterisation:

1.4.1. Mechanical testing:

An Instron 5566 equipped with a 500 N cell was used to measure tensile modulus (chord modulus between 0.05 and 0.25 % strain), strength, and strain at break based on the ASTM D638 protocol. The crosshead speed and gauge length were 50 mm/min and 50 mm, respectively.

1.4.2. Thermogravimetric analysis (TGA):

Mass loss curves of the blends were obtained by a thermogravimetry analyser (TA Instruments Q5000 IR thermogravimetric analyser). The sample in an alumina pan was heated at a constant rate of 10 °C/min from room temperature to 650 °C. All the samples were tested under air flow of 25 ml/min.

1.4.3. Differential scanning calorimetry (DSC):

The thermal behaviour of the samples was analysed in a TA Instruments Q1000 Differential Scanning Calorimeter (DSC). All the samples were heated to 250 °C with subsequent cooling to room temperature.

1.4.4. Fourier transform infrared spectroscopy (FT-IR):

FT-IR spectra of the samples were obtained in ATR mode on a Perkin Elmer Spectrum 100. For each sample, the spectra were averaged over 16 scans in the 600 to 4000 cm^{-1} range with a resolution of 4 cm^{-1}.

1.4.5. Scanning electron microscopy (SEM):

The morphology i.e. the fractured surfaces of the samples were observed through SEM (FEI Magellan 400 field emission XHR-SEM) without any sputter coating. The working distance ranged from 2.6 to 5.5 mm depending on the shape of the sample and the voltage used was 2 kV.

1.4.6. Cone calorimeter:

The reaction-to-fire properties of the samples were determined in a Dual cone calorimeter (Fire testing technology). Rectangular samples of dimensions 100 × 100 × 2 mm were subjected to a heat flux of 50 kW/m^2 until flameout. The standard used for the test was ISO 5660-1:2002. The conditions were: ambient temperature: 30 °C - 32 °C and air humidity: 31 % - 32 %.

2. Results and discussion:

2.1. The forming of the samples and their analyses:

It is to be noted that out of all the samples, the only ones that could be successfully formed were BC_Lanosol_WG_COMP and BC_APP_WG_COMP. Only these two samples were subjected to mechanical and fire testing. The other samples, including the aforementioned two, were subjected to TGA, DSC, FT-IR and SEM and the reason why the other samples did not 'form' successfully in the processing methods are explained subsequently.

2.2. Reaction-to-fire properties:

Fig. 3 shows the heat release curves of the samples that were successfully formed along with their corresponding neat polymers (without any FR doped biochar) as determined through a cone calorimeter. Table 1 shows the reaction-to-fire properties of the samples with their corresponding neat polymers. From Fig. 3, it can be seen that the addition of lanosol has reduced the PHRR of neat WG and the details are provided in section 2.3. of part 1 of this project report. Interestingly, when the biochar was doped with APP, the PHRR was significantly lowered resulting in a broad peak. The PHRR of BC_APP_WG_COMP sample was 186 kW/m^2, which was a substantial improvement from the 652 kW/m^2 of the neat WG and 636 kW/m^2 of the BC_Lanosol_WG_Comp sample. The TTI of BC_APP_WG_COMP was also the highest amongst the WG-based sample. Due to the broad nature of the heat release peak, the TPHRR was also delayed at 118 s. However,

the THR (i.e. the area under the heat release curve) of this sample was the highest because of the prolonged albeit non-intensive burning. The FPI is an indicator of tendency to flashover. The higher FPI values specify a higher fire retardancy performance and from Table 1, the WG-based sample having APP doped biochar had significantly higher FPI than the other WG-based composites. Table 1 also specifies the fire growth rate index (FIGRA) of the tested samples, and it is the growth rate of the burning intensity or heat release during a cone calorimeter (or other fire tests) test. FIGRA is also the maximum of the heat release rate of the tested divided by time [2]. The FIGRA of the BC_APP_WG_COMP sample was the lowest amongst the WG-based samples indicating that it is less likely to allow detrimental growth of fire. The neat PA 11 had a moderately high PHRR at 535 kW/m^2.

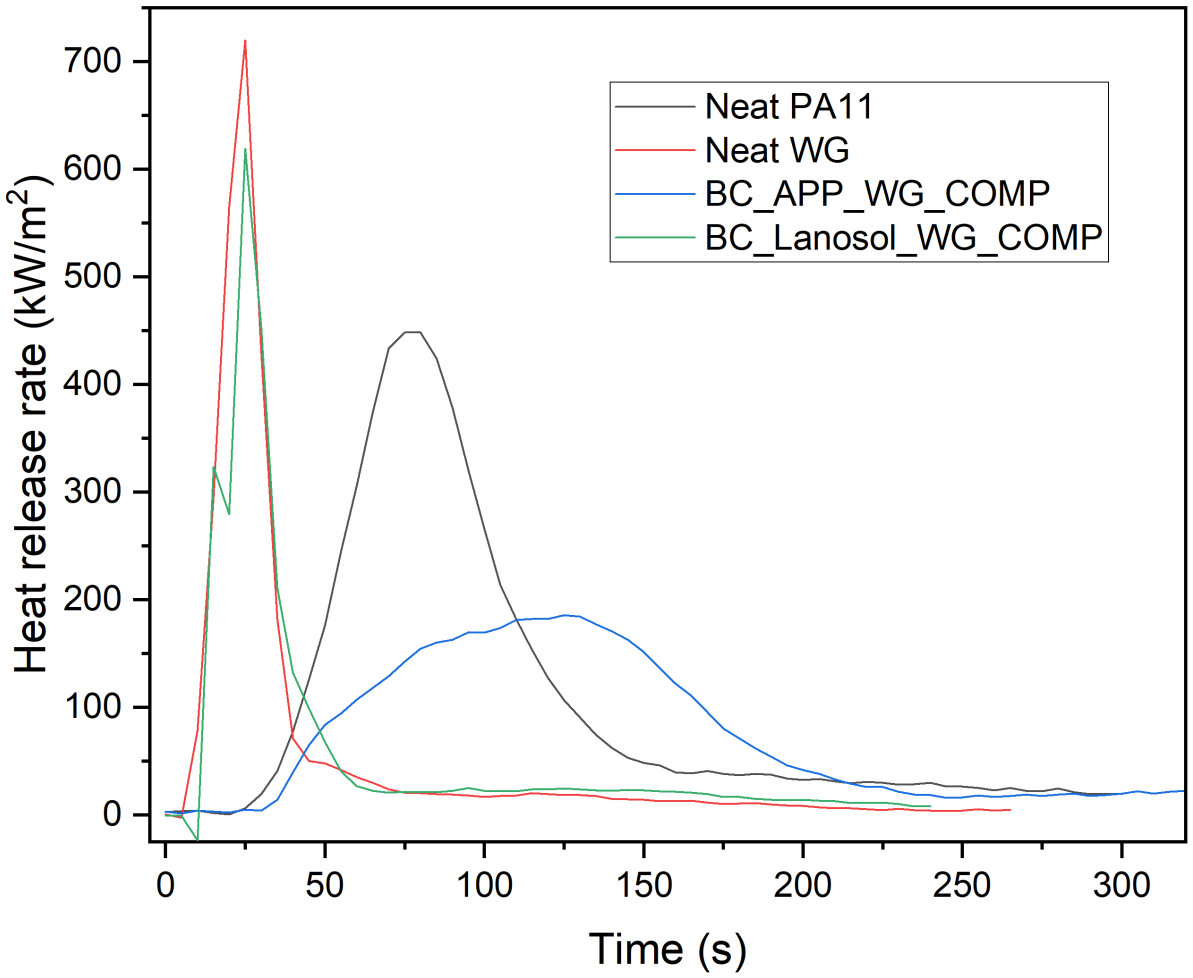

Fig. 3. Heat release curves of various samples obtained from cone calorimeter

Comparing lanosol-doped biochar and APP-doped biochar, the latter clearly performed better in the WG system both in the heat release profile with a broad peak and having superior reaction-to-fire parameters. The effect of lanosol on WG has been described in detail in part 1 of this report, wherein it aids in radical scavenging in the combustion regime. APP, on the other hand, acts in the condensed phase to create char as well as the nitrogen containing gases from the ammonia helps in the intumescence. WG, being a nitrogen protein, already is prone to charring during burning

and APP enhances this charring effect, which is the reason for a better fire performance that the composite having lanosol-doped biochar [3]. Additionally, the polyphosphoric acid, produced from the decomposition of APP at high temperatures reacted with the hydroxyl and amine groups in WG further reducing the combustion rate of the composite [4]. Thus, the reactive nature of APP and its tendency to cause an expanding char were the main reasons for the sample with APP performing better under radiative heat that the composite containing lanosol. Only one other study [5] has been identified where APP was used in protein-based bioplastics (in this case, Zein-based bioplastic). The PHRR was very similar to the current study although the amount of APP was 10 wt% as opposed to 15 wt% in the current study, which corroborates the methods adopted in this project. The authors of that study, unlike the current one, observed multiple peaks in the heat release curves. Based on these observations, APP was selected as the most suitable FR and further composites were designed with APP.

Table 1: Reaction-to-fire properties of various samples determined from cone calorimeter

Sample	PHRR [kW/m^2]	TPHRR [s]	TTI [s]	THR [MJ/m^2]	FPI [m^{2}s/kW]	FIGRA [kW/ms]
Neat WG	652 ± 38	25 ± 15	23 ± 4	13.1 ± 7.0	0.038 ± 0.01	26 ± 0.5
BC_Lanosol_WG_COMP	636 ± 24	23 ± 3.5	13 ± 2.8	11.5 ± 1.3	0.035 ± 0.02	28.3 ± 0.3
BC_APP_WG_COMP	186 ± 0.2	118 ± 10.6	27.5 ± 3.5	58.04 ± 5	0.63 ± 0.06	1.6 ± 0.14
Neat PA 11	535 ± 122	80 ± 7	20 ± 0	37.2 ± 6.2	0.155 ± 0.02	6.64 ± 0.9

2.3. Mechanical properties:

Table 2 summarises the mechanical properties of the formed samples. The effect of lanosol-doped biochar on the mechanical properties of WG is explained in section 2.1 of part 1 of this project report. Considering the standard deviation, the APP-doped sample has similar tensile strength as the neat WG and the sample containing lanosol-doped biochar. However, the ductility of the APP-doped sample is significantly lower than the other WG-based samples and this because of high amount of biochar and APP in the resin matrix that reduces polymeric chain mobility [6]. This is also the reason for this sample's lower toughness as indicated by low value of energy at break. A previous study by Verdolotti et al. [5] used APP (without the use of any biochar) in zein-based composites, which is analogous to WG because both of them are proteinaceous. The authors reported tensile strength of less than 1.5 MPa for both 10 and 30 wt% APP application in zein-based composites, which is significantly lower than what was achieved in the current study. Thus, it shows that doping of FR (regardless of lanosol or APP) in biochar helps to conserve the tensile strength of polymeric composites, while enhancing the fire performance (as seen in the fire testing in the current study). The neat PA 11 had a tensile strength of 42.5 MPa and modulus of ca. 1 GPa, which is similar to previously reported studies and data sheets [7, 8, 9].

Table 2: Mechanical properties of various composite samples.

Sample	Maximum tensile strength [MPa]	Modulus of elasticity [MPa]	Energy at break [J]	Elongation at break [mm/mm]
Neat WG	5.4 ± 0.1	277.2 ± 32.5	0.61 ± 0.1	0.35 ± 0.23
BC_Lanosol_WG	5.2 ± 0.3	265.6 ± 27	0.68 ± 0.2	0.34 ± 0.17
BC_APP_WG	3.6 ± 1.5	-	0.03 ± 0.02	0.053 ± 0.027
Neat PA 11	42.5 ± 4.0	1093 ± 77.3	0.01 ± 0.0	36.5 ± 14.0

2.4. Processing issues:

Certain samples were not able to be formed through compression and injection moulding techniques. Specifically, the BC_APP_PA 11_COMP was attempted to be compression moulded whereas injection moulding was tried on BC_APP_WG_INJ. In the case of BC_APP_PA 11_COMP the sample failed to fuse resulting in the plate getting shattered without any externally applied forces, as seen in Fig. 4. From Fig. 4., it can be seen that the vertical heat transfer was good, resulting in a cohesive 'forming' in the vertical direction. However, in the horizontal direction, the sample did not fuse. It is speculated this could be due to the high amount of heat shielding biochar in the sample, which hindered the flow of the melt more in the lateral direction than the vertical. Different compression moulding conditions were used to alleviate the aforementioned situation but yielded the same result as seen in Fig. 4. Thus, PA 11 was deemed to be an unsuitable bioplastic for this particular blend because the APP-doped biochar in WG was successfully compression moulded. Therefore, further manufacturing was conducted with WG as the selected bioplastic.

Fig. 4. The BC_APP_PA 11_COMP sample right after compression moulding. The sample inherently did not fuse and when it was taken out of the mould, the plate shattered. Several attempts gave the same result.

When the sample BC_APP_WG_INJ was attempted to be injection moulded, a similar issue happened wherein the sample was not cohesive having large through-and-through voids that hindered the formation of a 'whole' sample. Despite varying the injection time i.e. 3, 5, 15 and 20 s, the samples remained inconsistent, see Fig. 5. Hence, based on this, the injection moulding of APP-doped biochar in WG was considered to be unsuitable and compression moulding was identified as the preferred processing method for this type of formulation containing FR-doped biochars. Thus, based on the incremental experiments, the most suitable FR, bioplastic and processing method was APP, WG and compression moulding, respectively. This leads to the identification of a sample that as the best balance of fire-retardant and mechanical properties, which is APP-doped biochar in WG made by compression moulding or BC_APP_WG_COMP. Nevertheless, the samples (BC_APP_PA11_COMP and BC_APP_WG_INJ) that did not form in the aforementioned processing methods were still subjected to TGA, DSC, FR-IR and SEM analysis to identify their properties and get an insight into the reason for their inability to form through the applied processing techniques.

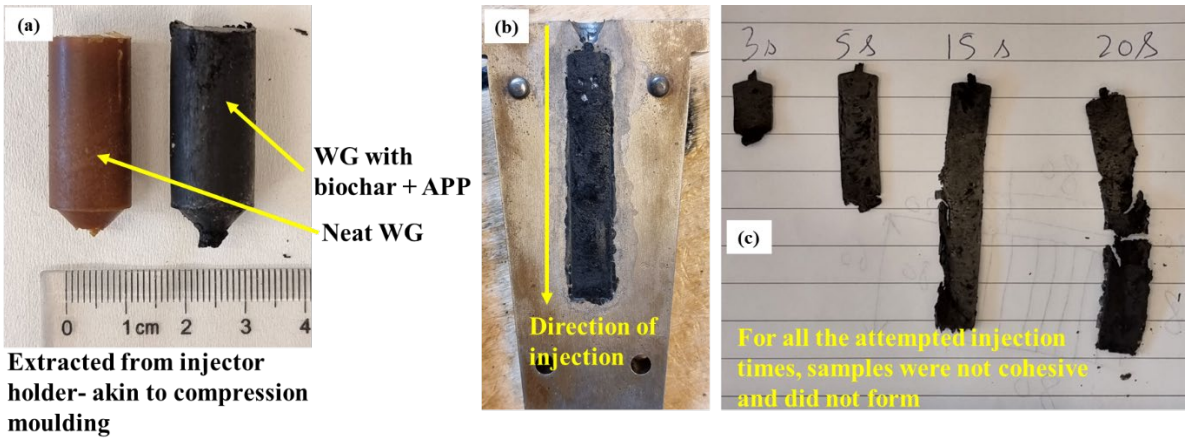

Fig. 5. The BC_APP_WG_INJ sample that failed to form into a cohesive sample.

2.5. Thermogravimetric analysis (TGA):

The mass loss curves of the samples as obtained from TGA analysis is shown in Fig. 6. Kindly note that all the samples were analysed, including the ones that formed and did not form using the processing techniques. Amongst the WG-based samples, the neat WG had the highest mass loss with residue of only ca. 18 % followed by the sample containing lanosol-doped biochar made by compression moulding and then the samples having APP-doped biochar (BC_APP_WG_COMP and BC_APP_WG_INJ). Additionally, the presence of APP had delayed the onset temperature of decomposition compared to the neat WG and the composite containing lanosol-doped biochar made using compression moulding. Hence, it is clear that APP is more efficient in inducing a beneficial thermal stability in the composites. In a previous study by Verdolotti et al. [5] where zein bioplastic (similar to WG) was analysed, the addition of 10 wt% APP with 3 wt% alkaline lignin increased the amount of residues remaining after the TGA test but the onset decomposition temperature did not change, compared to the neat polymer. Nevertheless, other studies have observed that the application of APP delays the onset decomposition temperature of the corresponding neat polymer [10, 11]. The reason for APP being better in imparting thermal stability in these WG composites compared to lanosol might be the same when it improved the reaction-to-fire properties. The reactive nature of APP along with its char forming ability induced

a heat shielding effect, which protected the virgin polymer from thermal decomposition. Neat PA 11 lost the most amount of mass and the addition of APP-doped biochar significantly improved both the onset decomposition temperature and the residue amount. It can also be inferred that the thermal stability is not affected by the processing method, for both WG and PA 11-based samples.

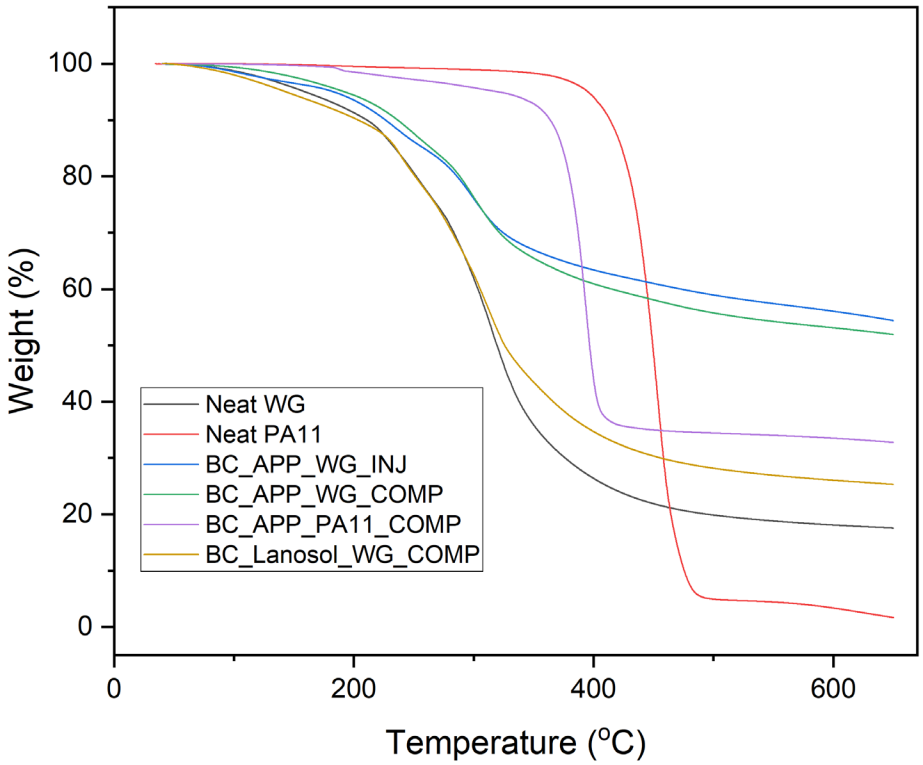

Fig. 6. TGA mass loss curves of all the composite samples and their corresponding neat polymers.

2.6. Differential scanning calorimetry (DSC):

The DSC curves of the composites are presented in Fig. 7. DSC was performed in order to gain an understanding, if possible, regarding the failure of certain mixes to form in the processing methods. For the PA 11-based samples, the neat polymer melts at ca. 190 °C, which is consistent with literature [12, 13] and crystallises at ca. 162 °C. However, when APP-doped biochar was added, the melting occurred somewhat earlier at a lower temperature compared to the neat PA 11. This could be due to the creation of small and flawed crystals structures that have lower melting temperature [14]. However, the crystallisation temperature was higher when doped biochar was included compared to the neat PA 11. This is due to the nucleation effect of the biochar particles, which acted as initiators for crystal growth [15, 16]. Despite this, no insight was able to be gained as to why the sample having APP-doped biochar in PA 11 failed to form in compression moulding. Similarly, the APP-doped biochar in WG made by compression and injection moulding was subjected to DSC to understand why compression moulding worked but not injection moulding. It is to be noted that in Fig. 7, the WG-based samples do not have a crystallisation peak because at or after ca. 150 °C, WG crosslinks, akin to a thermoset polymer. Regardless of the processing method, the melting temperature of the WG-based samples were similar. In fact, both BC_APP_WG_INJ and BC_APP_WG_COMP had almost the same thermal profile. Hence, the

reason for injection moulding not being able to form APP-doped biochar with WG needs to be evaluated with other means, such as electron microscopy as discussed subsequently.

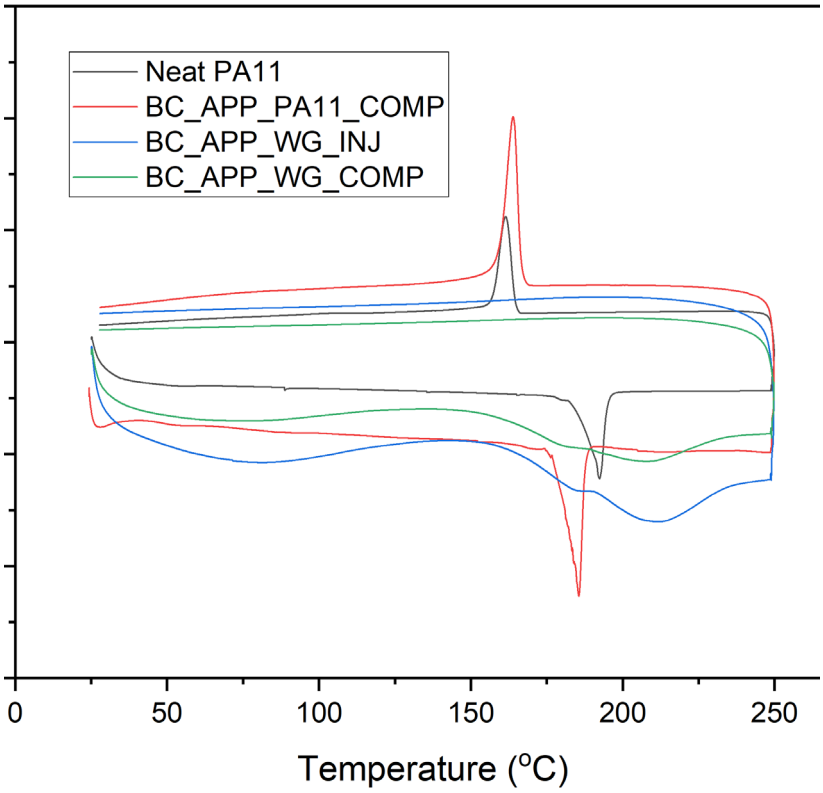

Fig. 7. DSC analysis of the composite samples.

2.7. Fourier transform infrared spectroscopy (FT-IR):

The FT-IR spectra of the composite samples are shown in Fig. 8. The FT-IR spectra of the composite samples are shown in Fig. 8. FT-IR analysis was carried out to gain a better understanding of the chemical modification in the fabricated composites. In the FTIR spectra of neat PA11, the peak at ca.1316 cm^{-1} corresponds to the N-H stretching. The peaks at ca. 1633 cm^{-1} correspond to the axial deformation vibration of C = O and ca. 1537 cm^{-1} correspond to the angular deformation vibration of NH, both are the typical peaks of PA11, i.e., amide I and amide II, respectively. The symmetric and antisymmetric stretching vibrations of C-H were observed at ca. 2850 cm^{-1} and ca. 2918 cm^{-1}, respectively, which are the intense peaks of PA. The symmetric angular deformations of CH_2 are represented by the peak at ca. 1465 cm^{-1} and ca. 1375 cm^{-1}. This agrees with the previous research done on PA11 [17]. The main characteristic peak of biochar was found in the BC_APP_PA11_COMP at ca. 980 cm^{-1}, indicating the presence of C-H stretching vibrations in the aromatic ring. This can be confirmed through the FT-IR peaks of biochar/polypropylene composites developed by Zhang et al. [18]. The addition of biochar changed the position and magnitude of the PA peak characteristic in the region between ca. 739 to 1263 cm^{-1}, indicating ineffective cohesion between PA and biochar. Barczewski et al. [19] found similar results on biochar/PP composites.

The compression moulded and injection moulded biochar wheat gluten composites are having similar FTIR spectra. A medium intensity peak was observed between ca. 1565-1700 cm^{-1} and a weak intensity peak at ca. 1475 to 1560 cm^{-1}, which correspond to the vibrational stretching of amide I (C=O) and the vibration frequency of amide II (N-H), respectively. Another medium intensity peak was observed at ca. 1430-1480 cm^{-1} corresponds to the amide III. The broad hydroxyl (OH) band was observed at ca. 3120-3315 cm^{-1}. The presence of the amide and broad hydroxyl (OH) band confirms the overall molecular conformation of the protein. Similar peaks have been noted in the investigation of Mohamed et al. [**20**]. In the region between ca. 745-1180 cm^{-1}, the intensity of the injection moulded composite was slightly increased when compared to compression moulded composite. This led to the conclusion that the manufacturing process has an impact on the characteristics of the resultant composite.

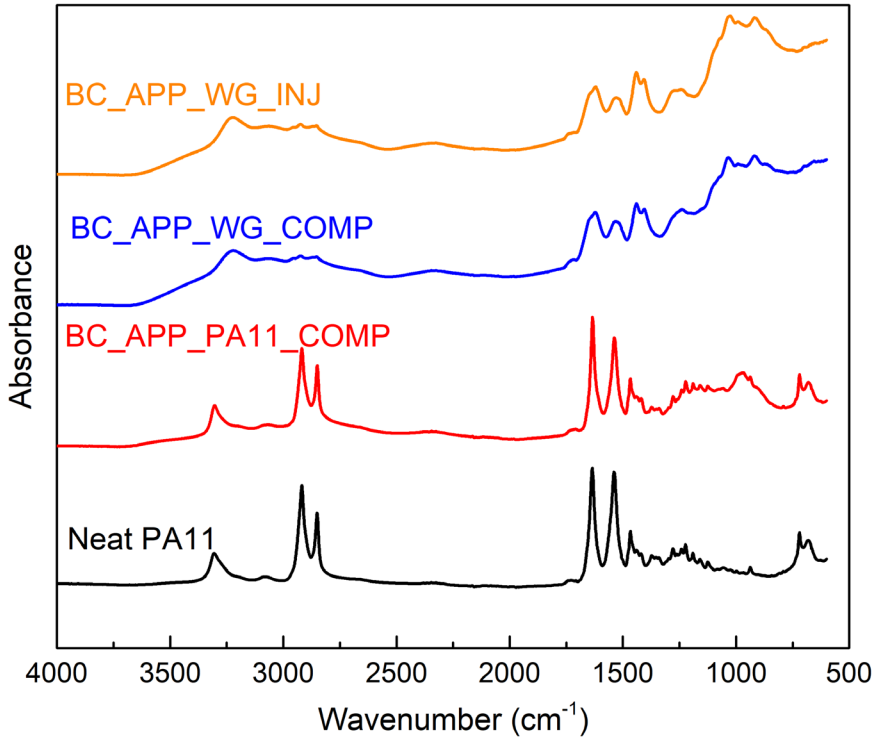

Fig. 8. FT-IR spectra of the composite samples.

2.8. Scanning electron microscopy (SEM):

The SEM micrographs of the composite samples are depicted in Fig. 9. The tensile fractured surface of neat PA 11 shows clear sign of ductile fracture with numerous fibril tears that coincides with the normal zone of the applied tensile stresses. However, when, APP-doped biochar was added to PA 11, the micrograph completely changed. The sample (BC_APP_PA 11_COMP) shows numerous chunks with clean edges, resembling small crystals. The presence of crystals was also observed in DSC when the crystallisation temperature increased compared to neat PA 11 due to the nucleation effect (see Fig. 7.). The BC_APP_WG_COMP sample shows that the APP was doped inside the biochar pores, as intended. However, it is to be kept in mind that the doping mechanism for lanosol and APP are different. Lanosol melts at ca. 124 °C whereas APP starts decomposing into ammonia and phosphoric acid at ca. 240 – 250 °C. Hence, it is plausible that phosphoric acid crystals were formed that were housed in the biochar pores along with APP. When

injection moulding is concerned, a polymeric material is subjected to shear forces [21]. In the micrograph of BC_APP_WG_INJ sample, large gaps can be observed in the polymer matrix as well as numerous crystals on the surface. As stated in section 2.4 of part 2, this sample was unable to fuse cohesively into the intended shape. The wide openings in the resin matrix seen in SEM could be the reason for the aforementioned and also the state of the injection moulded sample as shown in Fig. 5 b and c. It is speculated that the injection moulding induced shear forces have exposed the phosphoric acid crystals from the biochar pores, which might have hindered the fusing of the sample into the desired shape after cooling. Nevertheless, the BC_APP_WG_COMP sample exhibited the envisioned outcome wherein the APP was housed inside the biochar pores and exhibited low PHRR (186 kW/m^2) as seen in Fig. 3 and Table 1 of part 2.

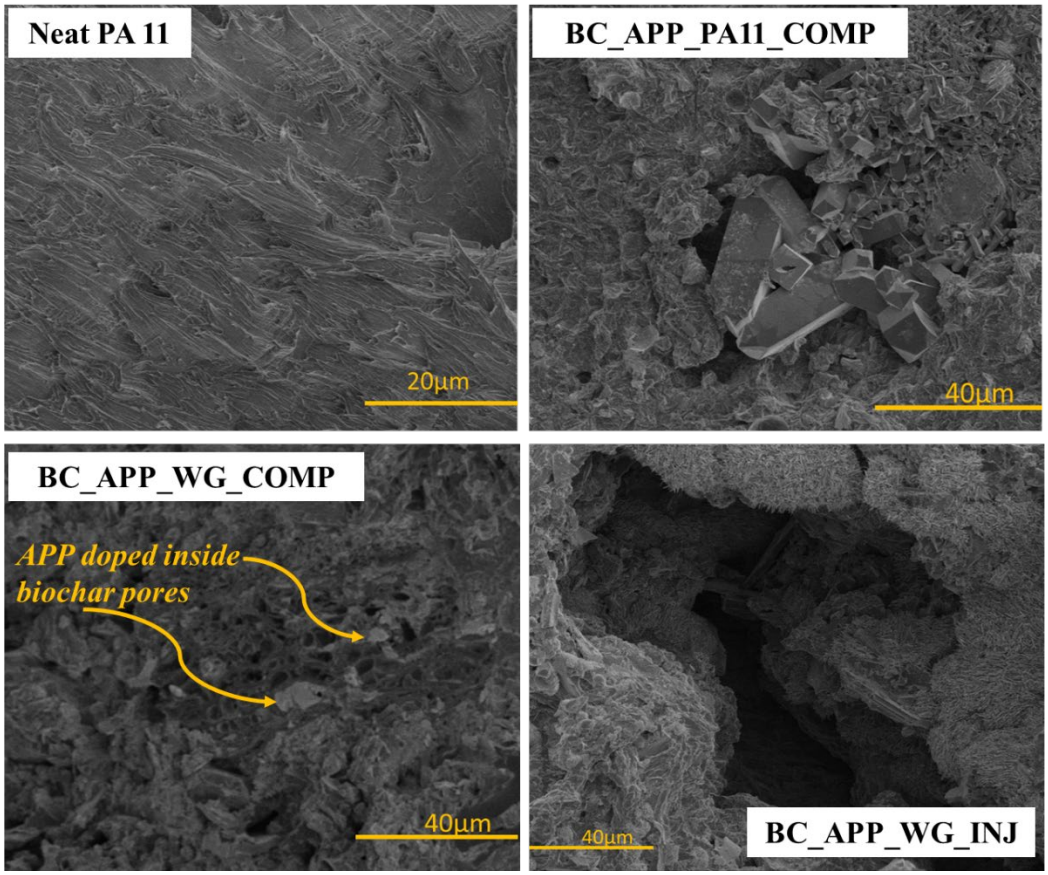

Fig. 9. SEM micrographs of the composites' fractured surfaces.

2.9. Kinetic analysis as activation energy:

According to Kumar et al. [22], the higher the temperature corresponding to 50 % weight loss ($T_{50\%}$) of the sample, the higher the activation energy required to break the bonds in the material. From the TGA results, $T_{50\%}$ of BC_APP_WG_COMP was measured to be 287.9 ^oC whereas that of BC_Lanosol_WG_COMP (i.e., the thermally doped lanosol in biochar and then added to lanosol followed by processing by compression moulding) was 300 ^oC. The temperatures indicate that more energy is required for the BC_Lanosol_WG_COMP composite to degrade compared to BC_APP_WG_COMP. The doping of lanosol into the pores of biochar as well as the crosslinking of the polymer chains in the BC_Lanosol_WG_COMP sample was more effective than doping

and compression moulding of BC_APP_WG_COMP. This could explain the higher decomposition temperatures and activation energy of BC_Lanosol_WG_COMP.

Concluding remarks for the entire project:

It has, since long, been established that the treatment of polymers with flame retardants improves the fire-safety properties and thermal stability, however, they tend to be detrimental to the mechanical performance. In light of the aforementioned issue, in this project, the effects of fire retardant-doped biochar on the mechanical and fire properties of two different bioplastics (wheat gluten and polyamide 11) made using two different processing methods (compression and injection moulding) were investigated. The aim of the project was to achieve a balance between the fire and mechanical properties in flame retardant-treated polymers, wherein the flame retardants (lanosol and ammonium polyphosphate) were doped into the pores of biochar to prevent stress concentration in the resin matrix. The work was divided into two parts where initially, the best doping method was identified using lanosol as the fire retardant, gluten as the bioplastic and compression moulding as the processing method. To make the wheat gluten composites, 4 wt% lanosol was doped into 6 wt% biochar using mechanical (dry mixing), chemical, and thermal doping techniques. The results showed that the new approach for improving the fire-resistant properties of gluten bioplastics was successful in that it preserved the mechanical strength. The thermal and chemical doping techniques were found to be the most effective in placing a significant amount of lanosol inside the biochar pores. The addition of un-doped biochar to the bioplastic increased the tensile strength and modulus the most. However, the thermally and chemically lanosol-doped biochar composites were able to retain the strength of the neat gluten bioplastic with a higher modulus. On the other hand, the addition of doped biochar to gluten reduced its ductility, which was expected. However, the material was still quite ductile. The thermogravimetry analysis of the samples showed a higher residue and slower decomposition rates for the doped samples compared to the neat gluten, thus, the stability of the gluten, over the full temperature range, was enhanced after doping. Additionally, from the microscale combustion calorimeter experiments, it was observed that the doped samples had lower peak heat release rate, peak combustion rate, heat release, and ignition capacities than the neat gluten, indicating an improvement in fire properties. In general, all the doping methods reduced the peak heat release rates of neat gluten with the thermally doped sample exhibiting the lowest value. Moreover, the structural integrity of the char residue, in the thermally doped sample, was preserved after the cone calorimeter test, confirming the effectiveness of the doping process. From kinetic analysis it was found that the same sample had the highest activation energy and the lowest ignition and fire growth capacities. Hence, based on the results of the various tests, it can be concluded that thermally doping lanosol into biochar is the most feasible method to impart fire retardancy and retain mechanical strength in gluten/protein-based bioplastics.

To observe if the new approach is effective in other polymeric systems, another set of experiments were conducted in part 2 of this project. In particular, 15 wt% ammonium polyphosphate as fire retardant was doped into 22.5 wt% biochar and tested in both gluten and polyamide 11 bioplastics. Additionally, the effect of processing methods i.e., compression and injection moulding were also determined. Wheat gluten and compression moulding were found to be the better bioplastic and processing method, respectively. The incorporation of biochar and ammonium polyphosphate in wheat gluten achieved a better fire performance (PHRR of 186 kW/m^2 and TTI of 28 s) compared to lanosol-doped sample (PHRR of 636 kW/m^2 and TTI of 13 s). Additionally, the tensile strength

of the lanosol-doped biochar in gluten made by compression moulding was 5.2 MPa while that of ammonium polyphosphate-doped counterpart was 3.6 MPa. Compared to the neat wheat gluten results (PHRR of 652 kW/m^2 and tensile strength of 5.4 MPa), the sample having lanosol-doped biochar in gluten made by compression moulding exhibited a balance between the mechanical and fire properties. Therefore, if fire retardancy is the ultimate aim of the composite application with acceptable mechanical properties then ammonium polyphosphate doped biochar in wheat gluten composite will be the best option. However, with overall acceptable properties (both mechanical and fire), lanosol-doped biochar in wheat gluten composite will be appropriate.

References:

[1] Shukor, F., Hassan, A., Islam, M.S., Mokhtar, M. and Hasan, M., 2014. Effect of ammonium polyphosphate on flame retardancy, thermal stability and mechanical properties of alkali treated kenaf fiber filled PLA biocomposites. Materials & Design (1980-2015), 54, pp.425-429.

[2] Park, J.W., Lim, O.K. and You, W.J., 2020. Analysis on the fire growth rate index considering of scale factor, volume fraction, and ignition heat source for polyethylene foam pipe insulation. Energies, 13(14), p.3644.

[3] Das, O., Kim, N.K., Hedenqvist, M.S. and Bhattacharyya, D., 2019. The flammability of biocomposites. In Durability and Life Prediction in Biocomposites, Fibre-Reinforced Composites and Hybrid Composites (pp. 335-365). Woodhead Publishing.

[4] Camino, G., Grassie, N. and McNeill, I.C., 1978. Influence of the fire retardant, ammonium polyphosphate, on the thermal degradation of poly (methyl methacrylate). Journal of Polymer Science: Polymer Chemistry Edition, 16(1), pp.95-106.

[5] Verdolotti, L., Oliviero, M., Lavorgna, M., Iannace, S., Camino, G., Vollaro, P. and Frache, A., 2016. On revealing the effect of alkaline lignin and ammonium polyphosphate additives on fire retardant properties of sustainable zein-based composites. Polymer Degradation and Stability, 134, pp.115-125.

[6] Ho, M.P., Lau, K.T., Wang, H. and Hui, D., 2015. Improvement on the properties of polylactic acid (PLA) using bamboo charcoal particles. Composites Part B: Engineering, 81, pp.14-25.

[7] Oliver-Ortega, H., Granda, L.A., Espinach, F.X., Mendez, J.A., Julian, F. and Mutjé, P., 2016. Tensile properties and micromechanical analysis of stone groundwood from softwood reinforced bio-based polyamide11 composites. Composites Science and Technology, 132, pp.123-130.

[8] Oliver-Ortega, H., Granda, L.A., Espinach, F.X., Delgado-Aguilar, M., Duran, J. and Mutjé, P., 2016. Stiffness of bio-based polyamide 11 reinforced with softwood stone ground-wood fibres as an alternative to polypropylene-glass fibre composites. European Polymer Journal, 84, pp.481-489.

[9] https://designerdata.nl/materials/plastics/thermo-plastics/polyamide-11?cookie=YES (Accessed: 25 August 2022).

[10] Das, O., Kim, N.K., Kalamkarov, A.L., Sarmah, A.K. and Bhattacharyya, D., 2017. Biochar to the rescue: Balancing the fire performance and mechanical properties of polypropylene composites. Polymer degradation and stability, 144, pp.485-496.

[11] Kim, N.K. and Bhattacharyya, D., 2016. Development of fire resistant wool polymer composites: Mechanical performance and fire simulation with design perspectives. Materials & Design, 106, pp.391-403.

[12] Bourmaud, A., Le Duigou, A., Gourier, C. and Baley, C., 2016. Influence of processing temperature on mechanical performance of unidirectional polyamide 11–flax fibre composites. Industrial Crops and Products, 84, pp.151-165.

[13] Jacques, B., Werth, M., Merdas, I., Thominette, F. and Verdu, J., 2002. Hydrolytic ageing of polyamide 11. 1. Hydrolysis kinetics in water. Polymer, 43(24), pp.6439-6447.
[14] Mago, G., Kalyon, D.M. and Fisher, F.T., 2011. Nanocomposites of polyamide-11 and carbon nanostructures: Development of microstructure and ultimate properties following solution processing. Journal of Polymer Science Part B: Polymer Physics, 49(18), pp.1311-1321.
[15] Das, O., Bhattacharyya, D., Hui, D. and Lau, K.T., 2016. Mechanical and flammability characterisations of biochar/polypropylene biocomposites. Composites Part B: Engineering, 106, pp.120-128.
[16] Jariyavidyanont, K., Focke, W. and Androsch, R., 2016. Crystallization kinetics of polyamide 11 in the presence of sepiolite and montmorillonite nanofillers. Colloid and Polymer Science, 294(7), pp.1143-1151.
[17] Bahrami, M., Abenojar, J. and Martínez, M.A., 2021. Comparative characterization of hot-pressed polyamide 11 and 12: mechanical, thermal and durability properties. Polymers, 13(20), p.3553.
[18] Zhang, Q., Khan, M.U., Lin, X., Cai, H. and Lei, H., 2019. Temperature varied biochar as a reinforcing filler for high-density polyethylene composites. Composites part b: engineering, 175, p.107151.
[19] Barczewski, M., Hejna, A., Sałasińska, K., Aniśko, J., Piasecki, A., Skórczewska, K. and Andrzejewski, J., 2022. Thermomechanical and Fire Properties of Polyethylene-Composite-Filled Ammonium Polyphosphate and Inorganic Fillers: An Evaluation of Their Modification Efficiency. Polymers, 14(12), p.2501.
[20] Mohamed, A., Finkenstadt, V.L., Gordon, S.H. and Palmquist, D.E., 2010. Thermal and mechanical properties of compression-molded pMDI-reinforced PCL/gluten composites. Journal of applied polymer science, 118(5), pp.2778-2790.
[21] Gedde, U.W., Hedenqvist, M.S., Hakkarainen, M., Nilsson, F. and Das, O., 2021. Applied polymer science (pp. 489-504). Springer.
[22] Kumar, V., Kumar, M. and Pugazhenthi, G., 2014. Effect of nanoclay content on the structural, thermal properties and thermal degradation kinetics of PMMA/organoclay nanocomposites. International Journal of Nano and Biomaterials, 5(1), pp.27-44.

Supplementary Information in relation to Part 1 of the final report for project number: 321-002; Functionalised biochar for fire-retardant and bio-based composites

Table S1: T_{ign}, IGC and FGC of WG and BWG composite

β/K s^{-1}	WG						BWG					
	Method A			Method B			Method A			Method B		
	T_{ign} (K)	IGC (J/g K)	FGC (J/g K)	T_{ign} (K)	IGC (J/g K)	FGC (J/g K)	T_{ign} (K)	IGC (J/g K)	FGC (J/g K)	T_{ign} (K)	IGC (J/g K)	FGC (J/g K)
0.5	134.3	272.3	261.7	235.4	44.6	153.5	131.3	42.9	165.8	246.7	30.4	95.3
1	120.8	86.5	199.5	234.5	45.4	131.4	130.9	109.9	239.9	209.8	67.7	158.4
1.5	116.3	183.7	316.8	228.1	61.6	157.2	122.7	138.8	268.2	224.3	65.8	138.6
2	127.9	147.2	267.5	227	58.7	150.8	126.02	166.6	302.4	220.1	65.6	161.0
2.5	130.6	142.0	256.5	238.5	55.9	160.2	133.2	138.6	255.4	221.3	64.3	160.7
3	131.7	142.9	260.3	232.1	57.4	156.8	129.5	143.3	257.4	231.6	65.9	164.9
3.5	134.1	137.6	243.5	242.6	56.6	144.1	134.6	140.5	258.6	233.6	60.2	150.6
4	136.5	141.0	257.8	247.9	58.4	164.1	134.8	140.2	248.6	240.5	59.5	148.1
4.5	134.4	142.6	256.6	244.1	59.0	165.0	138.8	139.9	243.0	239.9	61.6	154.9
5	136.1	141.2	249.1	246.4	57.0	153.9	133.5	149.7	252.5	230.5	64.5	159.4
5.5	132.14	134.1	229.7	246.1	57.6	163.1	137.3	141.6	235.6	237.9	61.6	159.2
Mean	**130.4 ±6.4**	**151.9 ±19.1**	**272.6± 21.3**	**238.4± 7.5**	**55.7± 5.5**	**154.6± 9.8**	**132.1± 4.7**	**132.1± 13.8**	**247.9± 18.2**	**230.6± 10.8**	**60.6± 2.8**	**150.1± 7.8**

Table S2: T_{ign}, IGC and FGC of LBWG and LWG composites

β/K s^{-1}	LBWG						LWG					
	Method A			Method B			Method A			Method B		
	T_{ign} (K)	IGC (J/gK)	FGC (J/gK)	T_{ign} (K)	IGC (J/gK)	FGC (J/gK)	T_{ign} (K)	IGC (J/gK)	FGC (J/gK)	T_{ign} (K)	IGC (J/gK)	FGC (J/gK)
0.5	114.3	57.9	186.6	215.77	62.8	139.4	118.8	45.9	147.7	235.3	113.8	215.4
1	128.9	103.3	209.9	233	63.6	155.4	117.6	85.6	169.1	233.3	49.1	107.8
1.5	108.9	105.9	212.5	256.6	65.1	147.9	117.3	106.6	193.1	240.7	58.1	132.7
2	116.7	108.1	204.8	248.9	67.2	150.6	116.1	113.0	184.7	299.6	45.7	119.5
2.5	115.8	134.3	237.2	251	64.5	147.8	121.5	124.3	207.3	241	57.7	140.8
3	120.6	127.3	244.1	251.6	65.9	145.9	125.5	120.2	205.4	250.4	56.8	141.7
3.5	118	119.7	210.1	189.7	96.6	187.9	125.8	123.4	220.3	251.4	51.5	130.1
4	121.7	127.4	212.9	260	63	154.6	127.3	120.7	198.7	251	51.6	125.4
4.5	122.5	118.9	201.2	260.3	59.9	151.3	127.5	122.2	195.7	248.4	51.7	130.5
5	118.9	132.4	199.1	-	-	-	133	120.2	197.8	253.1	50.1	121.7
5.5	130.4	121.2	211.2	-	-	-	125.7	132.9	206.4	-	-	-
Mean	**119.7± 6.2**	**114.2± 11**	**211.8±16.3**	**240.5±24**	**67.6± 11**	**153.4±13.8**	**123.3± 5.4**	**110.4±13**	**193.3±20**	**250.4± 18.7**	**58.6± 4.2**	**136.6± 10.7**

Table S3: T_{ign}, IGC and FGC of CLBWG and TLBWG composites

β/K s^{-1}	CLBWG						TLBWG					
	Method A			Method B			Method A			Method B		
	T_{ign} (K)	IGC (J/gK)	FGC (J/gK)	T_{ign} (K)	IGC (J/gK)	FGC (J/gK)	T_{ign} (K)	IGC (J/gK)	FGC (J/gK)	T_{ign} (K)	IGC (J/gK)	FGC (J/gK)
0.5	99.6	257.9	336.3	114.1	63.9	100.5	108.4	76.2	171.0	238.9	37.2	95.8
1	112.7	94.3	201.7	249.9	46.1	153.1	116	106.6	210.9	253.8	37.8	101.1
1.5	116.6	124.2	231.2	241.9	51.2	131.4	120.4	124.5	248.4	244.7	80.3	155.9
2	117	129.9	248.3	253.3	54.4	135.5	121.6	128.3	232.9	247	68.4	151.9
2.5	123.6	146.5	261.2	254.9	62.3	141.3	123.5	133.6	239.7	253.9	68.5	164.9
3	119	133.6	232.7	262.5	64.3	139.2	121.7	130.6	235.4	256.3	68.3	152.7
3.5	119.5	145.4	237.3	257.4	66.6	133.3	128.8	137.0	237.5	258	67.8	166.4
4	124.8	128.8	219.5	264	64.1	147.5	129.5	136.4	232.7	259.7	68.5	153.5
4.5	126.7	130.6	217.3	265.6	64.8	138.8	126.7	147.0	244.5	258.8	69.2	139.9
5	130.9	131.7	220.5	267.6	61.3	142.1	128	130.5	227.5	271.4	69.3	144.9
5.5	132.1	139.9	226.7	268.1	64.3	124.7	131.6	132.9	204.7	267	66.3	143.1
Mean	**120.2 ±6.4**	**142.1± 14.6**	**239.3± 16.8**	**245.4 ±8.6**	**60.3± 6.7**	**135.2± 8.1**	**123.3±5**	**125.8±10.4**	**225.9± 13.9**	**255.4 ±9.4**	**63.8± 13.5**	**142.8 ±9**

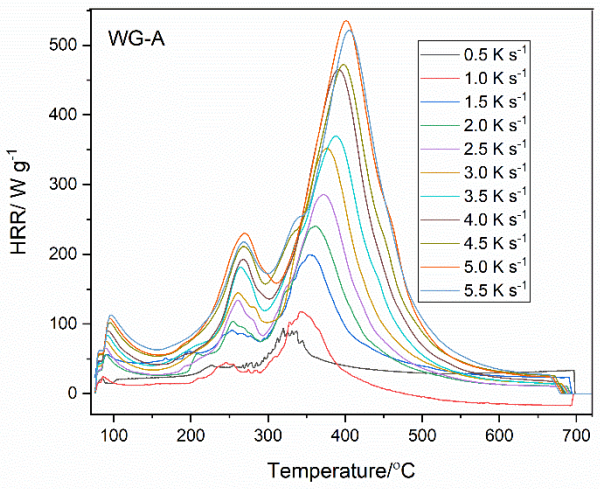
WG-A
HRR/ W g-1
Temperature/°C
0.5 K s-1
1.0 K s-1
1.5 K s-1
2.0 K s-1
2.5 K s-1
3.0 K s-1
3.5 K s-1
4.0 K s-1
4.5 K s-1
5.0 K s-1
5.5 K s-1

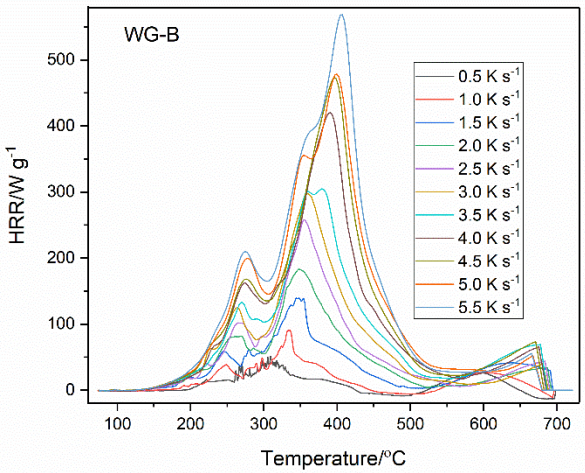
WG-B
HRR/W g-1
Temperature/°C
0.5 K s-1
1.0 K s-1
1.5 K s-1
2.0 K s-1
2.5 K s-1
3.0 K s-1
3.5 K s-1
4.0 K s-1
4.5 K s-1
5.0 K s-1
5.5 K s-1

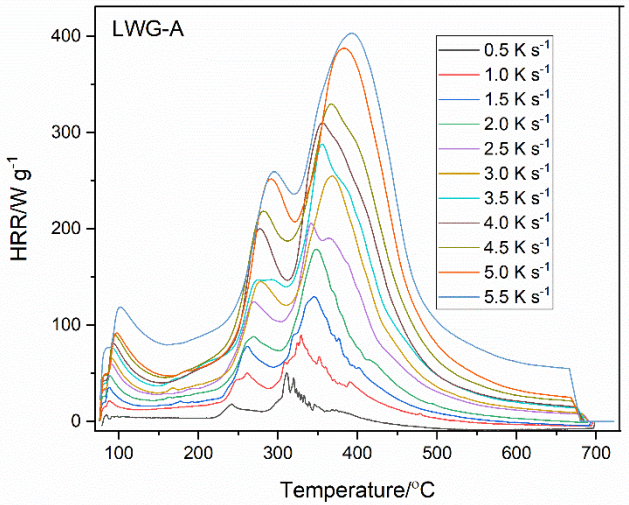
LWG-A
HRR/W g-1
Temperature/°C
0.5 K s-1
1.0 K s-1
1.5 K s-1
2.0 K s-1
2.5 K s-1
3.0 K s-1
3.5 K s-1
4.0 K s-1
4.5 K s-1
5.0 K s-1
5.5 K s-1

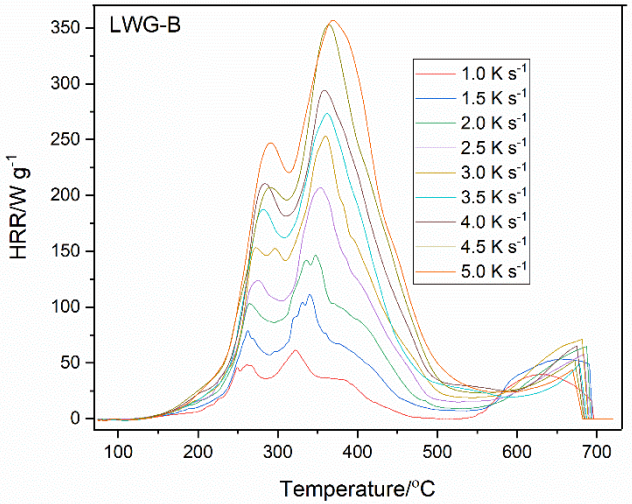
LWG-B
HRR/W g-1
Temperature/°C
1.0 K s-1
1.5 K s-1
2.0 K s-1
2.5 K s-1
3.0 K s-1
3.5 K s-1
4.0 K s-1
4.5 K s-1
5.0 K s-1

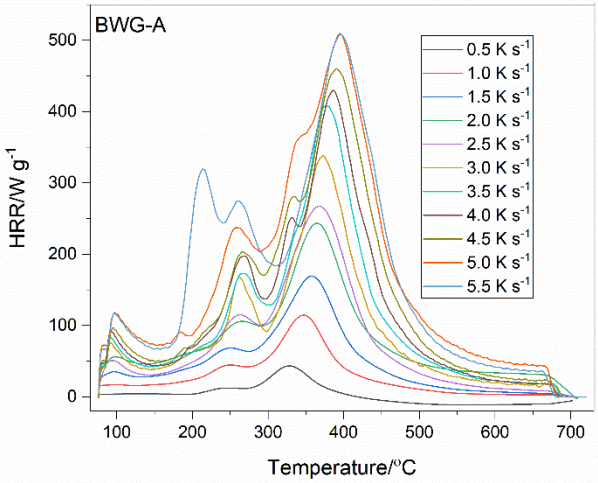
BWG-A
HRR/W g-1
Temperature/°C
0.5 K s-1
1.0 K s-1
1.5 K s-1
2.0 K s-1
2.5 K s-1
3.0 K s-1
3.5 K s-1
4.0 K s-1
4.5 K s-1
5.0 K s-1
5.5 K s-1

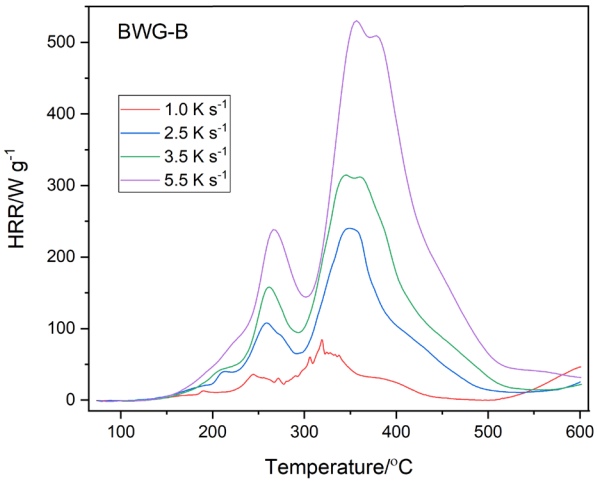
BWG-B
HRR/W g-1
Temperature/°C
1.0 K s-1
2.5 K s-1
3.5 K s-1
5.5 K s-1

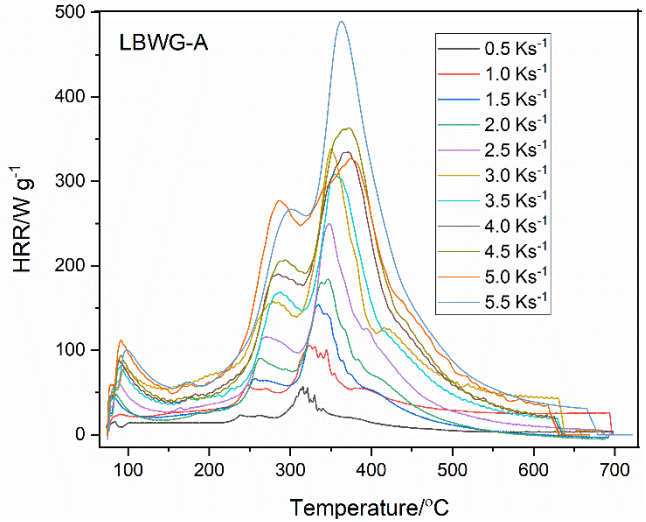

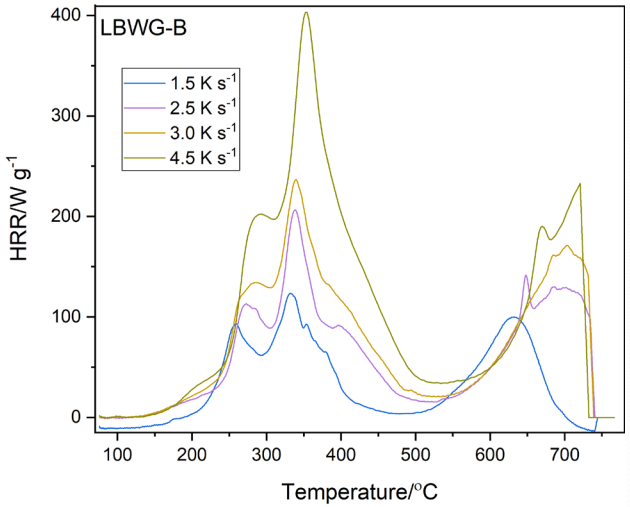

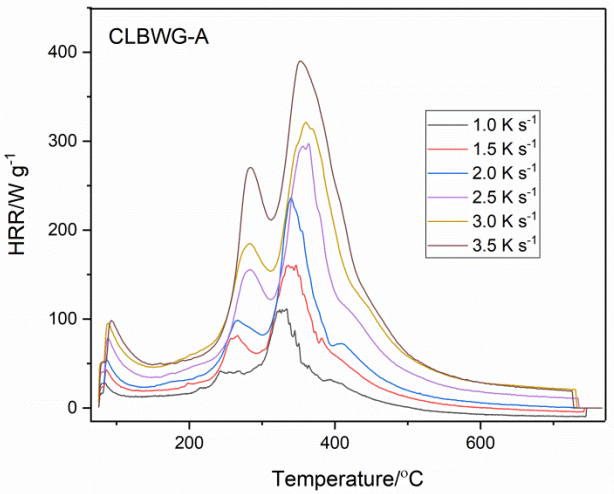

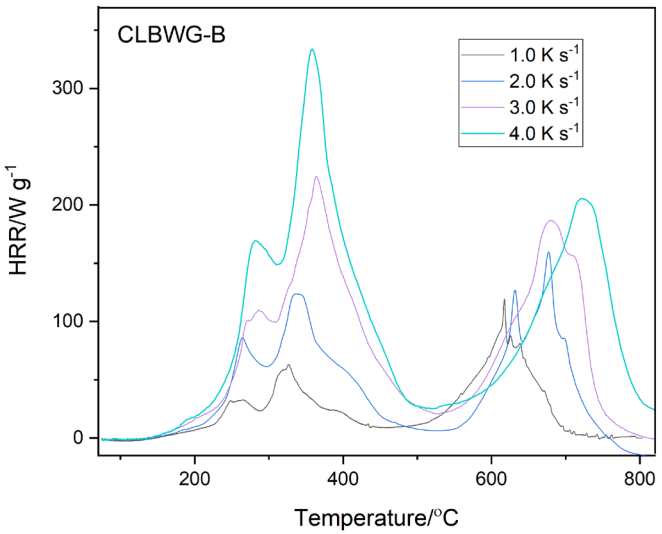

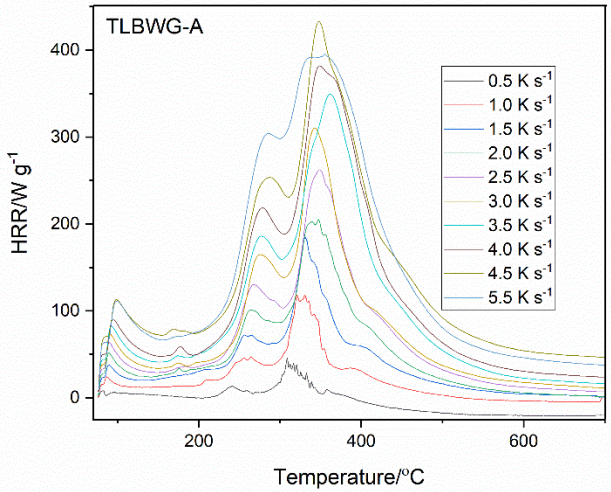

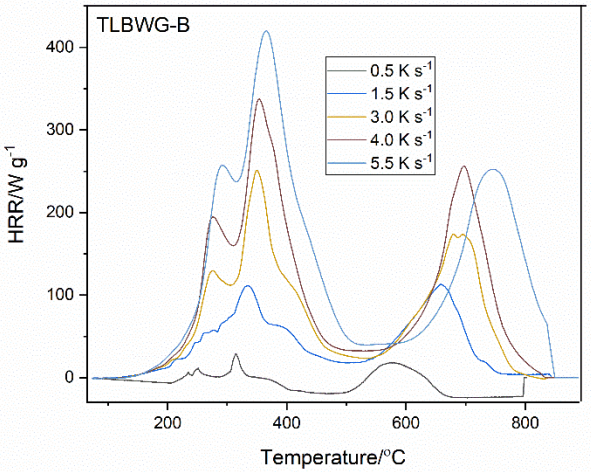

Fig. S1: Plots of heat release rate vs. temperature, from MCC test

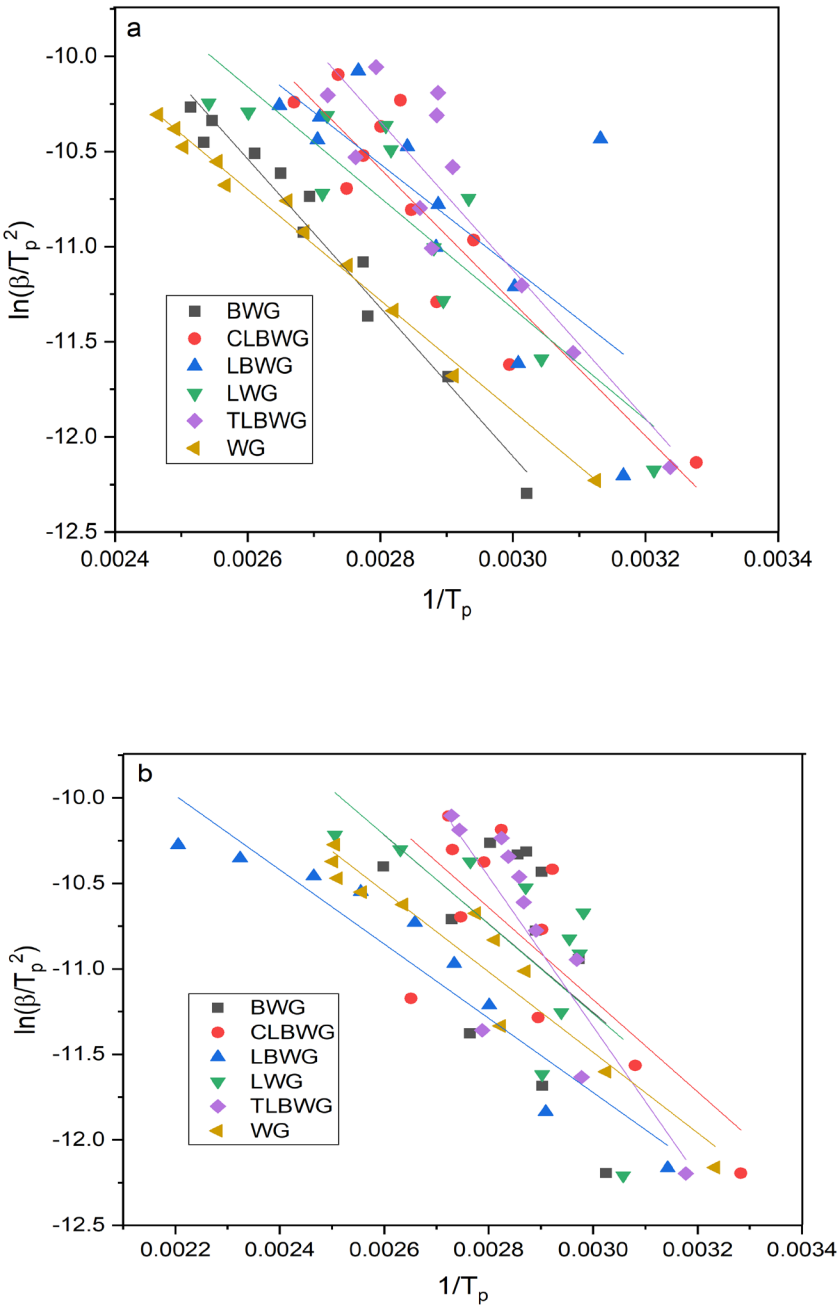

Fig. S2: Estimation of activation energy; a – Method A, b – Method B

Support organisations

This project was funded 2021 by the organizations below

Akademiska hus • Bengt Dahlgren Brand & Risk • BIV Föreningen för Brandteknisk Ingenjörsvetenskap • Brand och Bygg Sverige AB • Brandkåren Attunda Brandskyddsföreningen Gävleborg • Brandskyddsföreningen Skaraborg Brandskyddsföreningen Södermanland • Brandskyddsföreningen Värmland Brandskyddsföreningen Väst • Brandskyddsföreningen Västernorrland Brandskyddslaget • Dina Gruppen • Eld & Vatten • Folksam • Fortifikationsverket Försäkrings AB Göta Lejon • GellCon • If Skadeförsäkring • Kammarkollegiet Kingspan Insulation AB • Kiruna Räddningstjänst • Kristianstads Räddningstjänst Kommunassurans Syd Försäkrings AB • Kyrkans försäkring • Lantmännen MSB, myndigheten för samhällsskydd och beredskap • NBSG, Nationella Brandsäkerhetsgruppen • Nerikes Brandkår • Region Stockholm Trafikförvaltningen Riksantikvarieämbetet • RISE, Research Instiutes of Sweden AB • Räddningstjänsten Boden • Räddningstjänsten Kalix • Räddningstjänsten Karlstadsregionen Räddningstjänsten i F-län/Räddsam F • Räddningstjänsten Luleå • Räddningstjänsten Oskarshamn • Räddningstjänsten Skinnskatteberg • Räddningstjänsten Skåne Nordväst Räddningstjänsten Syd • Räddningsstjänsten Östra Götaland • Räddningstjänsten Mitt Bohuslän • Scania CV AB • S:t Erik Försäkrings AB • Sirius International Stanley Security • Statens fastighetsverk • Sparia Försäkringsbolag Stockholms Stads Brandförsäkringskontor • Storstockholms Brandförsvar Sveriges brandkonsultförening • Swedisol • Södertörns brandförsvarsförbund Södra Dalarnas Räddningstjänstförbund • Södra Älvborgs räddningstjänstförbund Trafikverket • Trygg-Hansa • Uppsala brandförsvar • Värends Räddningstjänst Västra Sörmlands Räddningstjänst • Östra Skaraborg Räddningstjänst

The Swedish Fire Research Foundation - enables development of fire safety knowledge by research and other activities, and the spread of this knowledge to make a difference in our society.

This is possible trough raising money from all kinds of organisations with fire safety on their agenda as well as for altruistic reasons. The broad support from our society together with prosperous networks are key factors for our success.

Our mission is "A sustainable and fire safe society built on knowledge"

Brandforsk
info@brandforsk.se, www.brandforsk.se

Project team

LULEÅ TEKNISKA UNIVERSITET

Financed by Brandforsk
Brandforsk's activities are made possible by support from various organizations in the community. Read more about our support organisations at www.brandforsk.se

BRAND FORSK